



DISSERTATION

Submitted to the
Combined Faculties for the Natural Sciences and for Mathematics of the
Ruperto-Carola University of Heidelberg, Germany
for the degree of
Doctor of Natural Sciences

Presented by
Haniyeh Sabouri Khameneh
Born in Tabriz (Iran)

Hyperforin induces senescence in endothelial and tumor cells

References:

1. Prof. Dr. Jonathan Paul Sleeman
2. Prof. Dr. Nicholas Foulkes

Oral examination:

24.06.2015

1 TABLE OF CONTENTS

SUMMARY	6
ZUSAMMENFASSUNG	7
LIST OF FIGURES	8
LIST OF TABLES	10
1 INTRODUCTION	11
1.1 Hyperforin	11
1.2 Historical perspective and definition of senescence	14
1.3 Hallmarks of senescent cells	15
1.3.1 Irreversible growth arrest	15
1.3.2 Altered cell morphology	15
1.3.3 Senescence-associated β -D-galactosidase activity	16
1.3.4 Altered gene expression and activation of tumor suppressor networks	17
1.3.5 Chromatin architecture and senescence associated heterochromatin foci (SAHF)	17
1.3.6 Autophagy	18
1.4 Senescence induction	18
1.4.1 DNA-damage induced senescence	18
1.4.2 Stress- induced senescence	19
1.4.3 Oncogene-induced senescence (OIS)	19
1.4.4 Tumor suppressor loss-induced senescence in vitro	19
1.5 Regulation senescence by signal transduction pathways	20
1.6 SIRT1 and senescence	23
1.7 Analysis of senescent cells	24
2 AIMS OF MY STUDY	26

3	MATERIAL AND METHODS	27
3.1	Materials	27
3.1.1	Instruments	27
3.1.2	Chemicals, reagents and consumables	28
3.1.3	Antibodies	31
3.1.3.1	Primary antibodies	31
3.1.4	Secondary antibodies	31
3.1.5	Cells	32
3.1.6	Buffers and solutions	33
3.2	Methods	36
3.2.1	DNA Quantification	36
3.2.2	Agarose gel electrophoresis	36
3.2.3	Preparation of CaCl ₂ competent E. coli cells	36
3.2.4	Transformation of competent E. coli cells	36
3.2.5	Isolation of plasmid DNA from E. coli cells	37
3.2.6	Cell culture methods	38
3.2.7	DNA plasmid transfection of cultured cells	39
3.2.8	RNA interference	39
3.2.9	Preparation of cell lysates	39
3.2.10	Protein concentration determination	39
3.2.11	SDS-PAGE and Western Blotting	40
3.2.12	FACS analysis	40
3.2.13	Senescence-associated-β-gal staining	41
3.2.14	In vivo experiments	41
3.2.15	Tissue Processing – OCT	41
3.2.16	X-gal staining in tissue	42
3.2.17	Cell death detection ELISA	42
3.2.18	Quantitative assay of senescence-associated β-galactosidase activity using cell extracts by MUG (4-Methylumbelliferyl β-D-Galactopyranoside)	42
3.2.19	Statistics	43
4	RESULTS	44
4.1	Senescence induction by hyperforin and aristoforin	44
4.1.1	Induction of senescence in endothelial cells	44
4.1.2	Antiproliferative potential of hyperforin against cancer cells is due in part to senescence induction	45
4.1.3	Senescence induction using hyperforin and aristoforin in different tumor cell lines	47
4.1.4	Hyperforin induces senescence in vivo	49

4.2	Molecular mechanism of hyperforin-induced senescence	50
4.2.1	Role of SIRT1	51
4.2.1.1	Effect of SIRT1 inactivation on senescence induction	53
4.2.2	Hyperforin induces Noxa expression at senescence-inducing concentrations	55
4.2.2.1	Knock down of Noxa expression by short hairpin ribonucleic acid (shRNA) suppresses hyperforin-induced senescence	57
4.2.2.2	Noxa induction by hyperforin is not dependent on p53	59
4.3	Development of improved methods to analyze senescent cells	62
4.3.1	Rapid flow cytometric method for measuring senescence associated beta-galactosidase activity using C ₁₂ -FDG	62
4.3.2	Quantification of FACS analysis of lysotracker yellow stained cells	63
4.3.3	Quantitative assay of senescence-associated β-galactosidase activity using cell extracts	64
5	DISCUSSION	66
5.1	Hyperforin induces senescence in ECs, tumor cell lines and tumors in vivo:	66
5.2	Molecular mechanism of hyperforin/aristoforin-induced senescence	68
5.2.1	Role of SIRT1	69
5.2.2	Downstream targets: Noxa and p53	71
5.2.3	Perspectives	72
6	REFERENCES	74
7	ACKNOWLEDGEMENT	83

SUMMARY

The limited life span of non-transformed somatic cells is largely due to the induction of replicative (telomere dependent) or premature (telomere independent) senescence. Senescence is a state of stable G1 arrest and thus represents a barrier to proliferation and transformation. Premature senescence is induced by several factors including stress, DNA damage and oncogenes. Senescent cell phenotypic changes include altered morphology, increased cell volume and increased natural senescence-associated β -galactosidase activity (SA- β -gal). Based on the results of previous studies, I hypothesized that hyperforin, a compound from St. John's Wort that has anti-cancer activity in vitro and in vivo, may exert its effects in part through the induction of senescence. In my thesis work I therefore aimed to determine whether hyperforin induces senescence in tumor and endothelial cells in vitro and/or in vivo, and if so to study the molecular mechanism by which hyperforin induces senescence. As a subsidiary aim I set out to establish novel methods for analyzing and quantifying senescent cells. I found that at low concentrations, hyperforin and its derivative aristoforin induce senescence in cultured endothelial cells and tumor cells, and also in tumor tissues, whereas at higher concentrations it induces apoptosis. Hyperforin inhibits SIRT1, but my results suggest that this only partially explains how hyperforin induces senescence. The senescence-inducing concentration of hyperforin is also able to induce Noxa expression in MCF-7 cells after 24h, 4 and 6 days. Importantly, in hyperforin-treated MCF-7 cells in which Noxa was knocked down, a significant reduction of senescence compared to hyperforin-treated control cells was observed. Hyperforin-induced Noxa expression was found to be independent of p53 expression, but p53 is required for senescence induction by hyperforin. In addition to these mechanistic studies, I also established an improved method for the detection of senescent cells. Together these findings show that induction of senescence by hyperforin is a novel anti-cancer mechanism that affects both tumor cells and endothelial cells, and strengthen the notion that hyperforin is a promising anti-cancer agent.

ZUSAMMENFASSUNG

Alle Zellen außer Tumorzellen haben eine beschränkte Lebensdauer, welche mit replikativer Seneszenz (Telomer-abhängig) oder frühzeitiger Seneszenz (Telomer-unabhängig) erklärbar ist. Replikative Seneszenz ist der Zustand der Zellen in der G1 Phase ohne Eintritt in die Zellteilungsphase und Transformation. Die frühzeitige Seneszenz wird durch mehrere Faktoren wie z.B. Stress, DNA-Schäden und Onkogene induziert. Die seneszenten Zellen zeigen phänotypische Veränderungen in der Morphologie. Sie zeigen gesteigertes Zellvolumen und eine erhöhte β -Galactosidase Aktivität. Aufgrund der Ergebnisse bisheriger Arbeiten, habe ich eine Hypothese aufgestellt. Dabei zeige ich wie Hyperforin, ein Präparat des Johanniskraut, das in vitro und in vivo Wirkung gegenüber Krebs zeigt, diesen Effekt zum Teil durch die Induktion der Seneszenz ausübt. In meiner Arbeit habe ich mir daher vorgenommen zu untersuchen, ob Hyperforin in Tumor- und Endothelzellen in vivo und in vitro Seneszenz induziert, und dabei den zugrundeliegenden Mechanismus aufzuklären. Um die Seneszenz der Zellen zu analysieren und quantifizieren zu können, habe ich als ergänzendes Ziel neue Methoden etabliert. Ich habe festgestellt, dass Hyperforin und ebenso dessen Derivat Aristoforin in niedriger Konzentration Seneszenz in kultivierten Endothel- und Tumorzellen induziert, aber auch in Tumorgeweben funktioniert. In höherer Konzentration wird dagegen Apoptose induziert. Auch beim SIRT1-Knockdown wird durch Hyperforin eine signifikante Steigerung der Seneszenz hervorgerufen. Weiterhin wird durch Hyperforin nach 24 Stunden, 4 und 6 Tagen die Expression von Noxa in MCF-7 Zellen induziert. Interessanterweise wurde, im Vergleich zu mit Hyperforin behandelten Kontrollzellen, in Abwesenheit von Noxa eine signifikante Reduktion der Seneszenz beobachtet. Hyperforin induzierte Noxa-Expression ist dabei p53 unabhängig, wobei p53 allerdings für die Induktion der Seneszenz durch Hyperforin benötigt wird. Zusätzlich gelang es mir zu diesen mechanistischen Studien eine bessere Methode zur Detektion von seneszierenden Zellen zu etablieren.

Es wurde gezeigt, dass die Induktion von Seneszenz durch Hyperforin ein neuartiger Anti-Krebs-Mechanismus ist, der sowohl Tumor- als auch auf Endothelzellen beeinflusst. Diese Ergebnisse sprechen für den Anti-Krebs-Effekt von Hyperforin.

LIST OF FIGURES

FIGURE 1 - INHIBITION OF PROLIFERATION IN TUMOR CELL LINES BY HYPERFORIN	12
FIGURE 2 - HYPERFORIN AND ARISTOFORIN INHIBIT ENDOTHELIAL CELL PROLIFERATION	13
FIGURE 3 - SENESENCE-ASSOCIATED (SA)- β GAL STAINING IN HUVECS. SENESENCE CELLS SHOW FLATTENED STRUCTURE.....	16
FIGURE 4 - THE ROLE OF P53 IN CELLULAR SENESENCE.....	20
FIGURE 5 - PATHWAYS TO SENESENCE	22
FIGURE 6 - SCHEMATIC REPRESENTATION OF P53 ACETYLATION, MTOR ACTIVITY AND THE INDUCTION OF SENESENCE OR CELL CYCLE ARREST	23
FIGURE 7 - INDUCTION OF SENESENCE BY HYPERFORIN AND ARISTOFORIN IN HUVECS	45
FIGURE 8 - DOSE- AND TIME-DEPENDENT SENESENCE INDUCTION IN THE T47D CELL LINE VIA HYPERFORIN .	46
FIGURE 9 - DOSE- AND TIME-DEPENDENT INDUCTIONS OF APOPTOSIS USING HYPERFORIN IN T47D CELLS	47
FIGURE 10 - SENESENCE INDUCTION BY HYPERFORIN AND ARISTOFORIN IN DIFFERENT CANCER CELLS	48
FIGURE 11 - DETECTION OF X-GAL POSITIVE CELLS IN TUMOR TISSUE USING HYPERFORIN	50
FIGURE 12 - HYPERFORIN- AND ARISTOFORIN-INDUCED SENESENCE IS SUPPRESSED BY THE SIRTUIN ACTIVATOR RSV IN ECS.....	51
FIGURE 13 - HYPERFORIN- AND ARISTOFORIN-INDUCED SENESENCE CAN BE INHIBITED BY THE SIRTUIN ACTIVATOR RSV IN SOME CANCER CELLS.....	53
FIGURE 14 - WESTERN BLOTTING OF MCF-7 CELLS RELATED TO THE SIRT1 EXPRESSION BY HYPERFORIN TREATMENT.....	54
FIGURE 15 - KNOCKDOWN OF SIRT1 EXPRESSION IN MCF-7 CELLS DOES NOT INHIBIT HYPERFORIN-INDUCED SENESENCE	55
FIGURE 16 - WESTERN BLOT ANALYSIS OF NOXA EXPRESSION USING 8 MM HYPERFORIN AT LOW CONCENTRATION	56
FIGURE 17 - WESTERN BLOT ANALYSIS OF NOXA INDUCTION BY HYPERFORIN AND ARISTOFORIN AT LOW CONCENTRATIONS.....	57
FIGURE 18 - WESTERN BLOT ANALYSIS OF NOXA INDUCTION USING SHRNA AGAINST NOXA BY HYPERFORIN TREATMENT.....	58
FIGURE 19 - FUNCTIONAL ANALYSIS OF NOXA EXPRESSION	58
FIGURE 20 - HYPERFORIN AND ARISTOFORIN INDUCE SENESENCE IN A P53-DEPENDENT MANNER	60
FIGURE 21 - HYPERFORIN- AND ARISTOFORIN-INDUCED SENESENCE IN HCT+/- CELLS CAN BE INHIBITED BY THE SIRTUIN ACTIVATOR RSV	61
FIGURE 22 - QUANTITATIVE SA- β GAL ASSAY USING MUG.....	65

FIGURE 23 - SCHEMATIC REPRESENTATION OF MECHANISMS THROUGH WHICH HYPERFORIN AND ARISTOFORIN INDUCE SENESCENCE.....	69
---	----

LIST OF TABLES

TABLE 1 - QUANTIFICATION OF SENESCENT CELLS USING X-GAL STAINING, AND PARALLEL QUANTIFICATION OF C12FDG-STAINED CELLS USING FACS ANALYSIS	63
TABLE 2 - QUANTIFICATION OF FACS ANALYSIS USING LYSOTRACKER YELLOW AND X-GAL STAINING	64

1 INTRODUCTION

Normally, cells grow old and die after a certain time, for example through apoptosis, or through entering an irreversible non-dividing state called senescence. In cancer, somatic cells start to grow and divide in an unregulated manner, replacing and destroying healthy tissue. Understanding how senescence is induced may identify novel ways of inhibiting the proliferation of cancer cells. Furthermore, tumor growth requires the formation of new blood vessels that sprout from pre-existing vessels in the process of angiogenesis to nurture tumor cells (Folkman, 1995). Lymphangiogenesis, the new growth of lymphatic vessels, also stimulates metastasis formation (Ohta et al, 2000). As blood and lymphatic vessels are lined with endothelial cells (ECs), induction of senescence in ECs may also inhibit tumor development and metastasis by suppressing angiogenesis and lymphangiogenesis, respectively (Vogel et al, 2007). The focus of this study was to determine whether senescence is induced in endothelial and tumor cells in response to hyperforin treatment, and if so, to determine the molecular mechanisms through which it exerts these effects. Understanding the molecular mechanisms through which hyperforin induces senescence may provide new insights into the process of senescence and its regulation, and possibly pave the way to new targets for cancer treatment.

1.1 Hyperforin

Hypericum perforatum is a perennial plant of the *Guttiferace* family (Medina et al, 2006). Some taxonomists classify the genus *Hypericum* in a separate family, the *Hypericaceae* (Arfan et al, 2009). From 400 species of the genus *Hypericum*, 10 species grow in central Europe (Hölzl, 1993). Hyperforin was first isolated in the 1960s due to its antibiotic activity against several gram-positive bacteria such as *Staphylococcus aureus* (Schempp et al, 1999). Hyperforin is poorly soluble and unstable in aqueous solution and is sensitive to light and oxygen, which limits its clinical potential. Therefore, a stable and more hydrophilic chemical derivative, aristoforin, has been synthesized (Gartner et al, 2005).

In the context of cancer, hyperforin inhibits matrix proteinases, tumor invasion and metastasis (Donà et al, 2004), and inhibits the proliferation of a number of

mammalian cancer cell lines as well as showing an antiproliferative effect on phytohemagglutinin-stimulated peripheral blood lymphocytes (Schempp et al, 2000); (Figure 1). In part, the anti-proliferative effect of hyperforin is due to the induction of apoptosis, as demonstrated in various types of tumor cells (Schempp et al, 2000; Merhi et al, 2011).

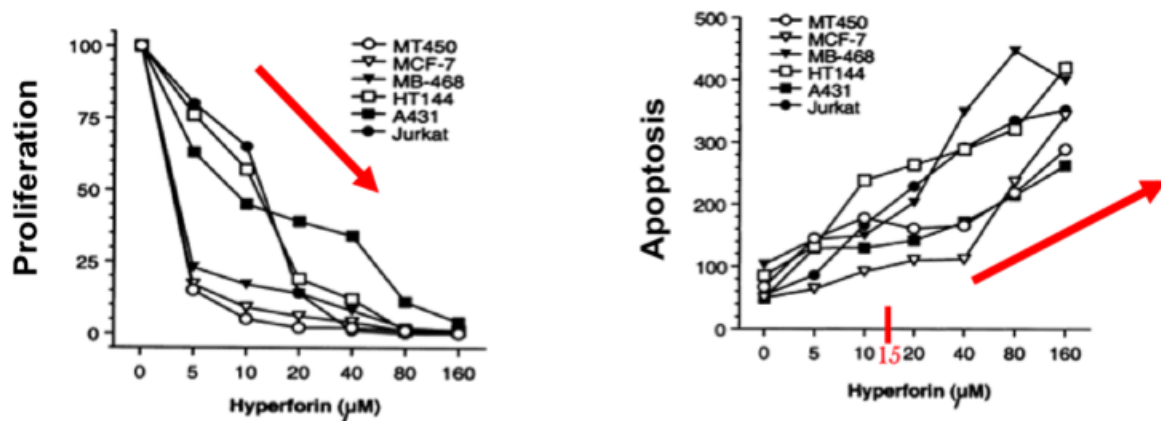


Figure 1 - Inhibition of proliferation in tumor cell lines by hyperforin

The growth of the tested tumor cell lines was inhibited by hyperforin, with IC_{50} values of 3-15 μM . At lower hyperforin concentrations, proliferation was inhibited largely in the absence of apoptosis. Above 15 μM hyperforin induced apoptosis (from Schempp et al, 2000).

At concentrations around 30 μM , hyperforin also induces apoptosis in lymphatic endothelial cells (LECs) (Rothley et al, 2009) in a dose-dependent manner (Figure 2). Importantly, hyperforin also inhibits the proliferation of LECs at lower concentrations (less than 10 μM) without inducing apoptosis, but rather by inducing cell cycle arrest, as assessed by flow cytometry (Rothley et al, 2009).

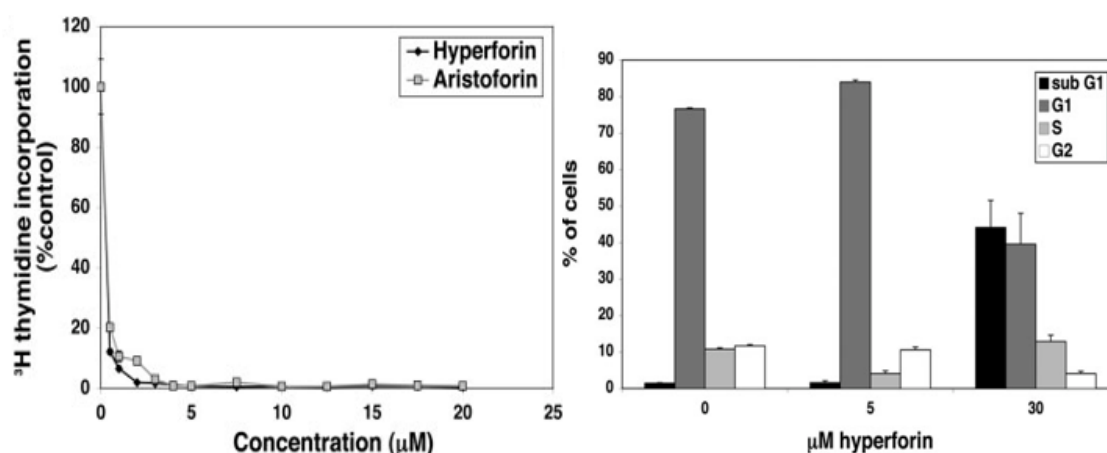


Figure 2 - Hyperforin and Aristoforin inhibit endothelial cell proliferation

The left graph shows the proliferation assay of LECs treated by hyperforin and aristoforin at different concentrations. Hyperforin and aristoforin inhibit proliferation at low concentrations (5 μM). The right graph shows cell cycle analysis of LECs untreated and treated with 5 and 30 μM hyperforin. Note that LECs treated with 5 μM hyperforin exhibit a reduced sub G1 and S phase level compared to 30 μM hyperforin (with permission of Rothley et al, 2009).

Mechanistically, hyperforin causes the release of cytochrome c from mitochondria and activates the mitochondria-mediated apoptosis pathway (Schempp et al, 2002). Accordingly, hyperforin induces cell death in primary malignant cells from patients with chronic lymphocytic leukemia through mitochondrial caspase-dependent apoptosis, which correlates with activation of the pro-apoptotic protein Noxa (Billard et al, 2003). Hyperforin inhibits the phosphorylation of Akt1 and thereby inhibits Bad, a direct downstream target of Akt1, by its dephosphorylation of Ser¹³⁶ (Martelli et al, 2006), which leads to apoptosis. Hyperforin changes the level of Ser¹³⁶-p-Bad but not the level of total Bad (Zhao et al, 2004), as well as levels of the anti-apoptotic Bcl-2, pro-apoptotic Noxa and caspase-9 and -3 in AML U937 cells (Merhi et al, 2011). In mammary carcinoma cells hyperforin also increases the activity of caspase-9 and -3 to induce apoptosis (Schempp et al, 2002). Furthermore, hyperforin was found to promote apoptosis in B-cell chronic lymphatic leukemia (B-CLL) cells, which leads to phosphatidylserine externalization and DNA fragmentation by caspase-3 activation (Quiney et al, 2006).

Hyperforin inhibits EC migration and invasion (Dona et al, 2004), an early step in the process of angiogenesis. It further inhibits the activity of urokinase, elastase and matrix metalloproteinase-2 and -9 (Carmeliet and Jain, 2000). The activation of NF-

kB, a transcription factor which regulates numerous genes involved in cell growth, survival, angiogenesis and invasion in endothelial cells is prevented by hyperforin (Noonan et al, 2011). In addition, hyperforin and aristoforin inhibit lymphangiogenesis in the thoracic duct ring outgrowth assay (Rothley et al, 2009). The observation that hyperforin at around 5 μ M inhibits proliferation but does not induce apoptosis suggests that hyperforin may lead to cell cycle arrest and promote senescence (Rothley et al, 2009). Altogether, these properties qualify hyperforin as a lead structure for the development of new therapeutic molecules in the treatment of malignant tumors (Quiney et al, 2006).

1.2 Historical perspective and definition of senescence

The basis of this study is the hypothesis that hyperforin can inhibit the proliferation of ECs and tumor cells by inducing senescence. The concept of senescence arose from the observation that primary cells isolated from tissues and grown in culture have a limited capacity to divide (Hayflick and Moorhead, 1961). Hayflick and Moorhead divided the stages of cell culture into three phases. When the cells cover the surface of the culture flask, they reach the first phase. The second phase represents the period when cells are dividing in culture and must be subcultivated to keep them growing. After some time, the cells stop dividing (growing) but remain vital, which marks the beginning of the third phase, which is characterized by replicative senescence (Hayflick, 1965). Replicative senescence has been found in many cell types such as keratinocytes, endothelial cells, lymphocytes, adrenocortical cells, vascular smooth muscle cells and chondrocytes. Replicative senescence is also detected in cells derived from embryos and adults of all ages (Hayflick, 1965), and is associated with progressive telomere shortening during each successive round of DNA replication (Frenck et al, 1998).

From an evolutionary perspective, cellular senescence has evolved as a mechanism to prevent the transmission of damaged DNA into the next generation (Carnes and Olshansky 1994). For example, activation of proto-oncogenes leads to the induction of senescence, which acts as a barrier to transformation (Campisi, 2001). Many cancer cells senesce either spontaneously or in response to extracellular stress stimuli (Benhar et al, 2002). Tumor cells are often resistant to apoptosis by anticancer treatment. Therefore, induction of senescence in tumor cells could be an

alternative approach in cancer therapy (Schmitt et al, 2002; Shay and Wright 2005). For example, in cancer cells, telomerase is an attractive target to induce senescence. Inhibition of telomerase in cancer cells leads to shortening of telomeres, which causes senescence (Harley, 1991; Kiyono et al, 1998; Bodnar et al, 1998).

1.3 Hallmarks of senescent cells

Senescent cells are identified *in vitro* and *in vivo* by a number of characteristics, including irreversible growth arrest, altered cell morphology, senescence associated β -galactosidase activity, activation of tumor suppressor networks and altered gene expression, senescence associated heterochromatic foci (SAHF) and autophagy (Muller et al, 2009). These characteristics can be identified using specific biomarkers.

1.3.1 Irreversible growth arrest

The most obvious hallmarks of senescent cells are growth arrest, inability to replicate DNA and lack of responsiveness to physiologic mitogenic stimuli (Cristofalo, 1993). Senescent cells experience growth arrest in the transition from phase G1 to phase S of the cell cycle (Sherwood et al, 1988). In contrast to early passage human diploid fibroblasts (HDFs), late passage senescent HDFs do not respond to epidermal growth factor (EGF), tumor necrosis factor alpha (TNF- α), fibroblast growth factor (FGF) or interleukin-1 (IL-1) (Cristofalo, 1973). The quantification of newly synthesized DNA in the cell cycle can be performed using 5-bromo-2-deoxyuridine or [3 H]-thymidine-incorporation assays, thus enabling the researcher to distinguish arrested and senescent cells from dividing cells. Cellular senescence both *in vitro* and *in vivo* can also be identified using cell cycle biomarkers associated with senescence. Unfortunately, none of these biomarkers detect only senescent cells. For example, p16 and p21 are not specific for senescence but are also cell cycle arrest biomarkers (Campisi, 2007).

1.3.2 Altered cell morphology

Senescent cells have a flattened or thin cytoplasm (Figure 3). The expression of actin and tubulin is downregulated, while the synthesis of vimentin dramatically increases (Hay and Strehler, 1967; Lima and Macieira, 1972). Furthermore, the size of senescent cells is larger as compared to pre-senescent cells (Figure 3). For example, a flat cell phenotype is seen in cells undergoing H-RAS^{V12} induced-senescence

(Serrano et al, 1997), stress-induced senescence (Parrinello et al, 2003) or DNA-damage-induced senescence (Chen et al, 1995). Senescent cells frequently develop abnormal nuclei or a multi-nuclear phenotype due to genomic instability (Matsumura et al, 1979). Additionally, caveolin-1 plays an important role in the morphological changes of senescence by regulating focal adhesion kinase activity and actin fiber formation (Cho et al, 2004).

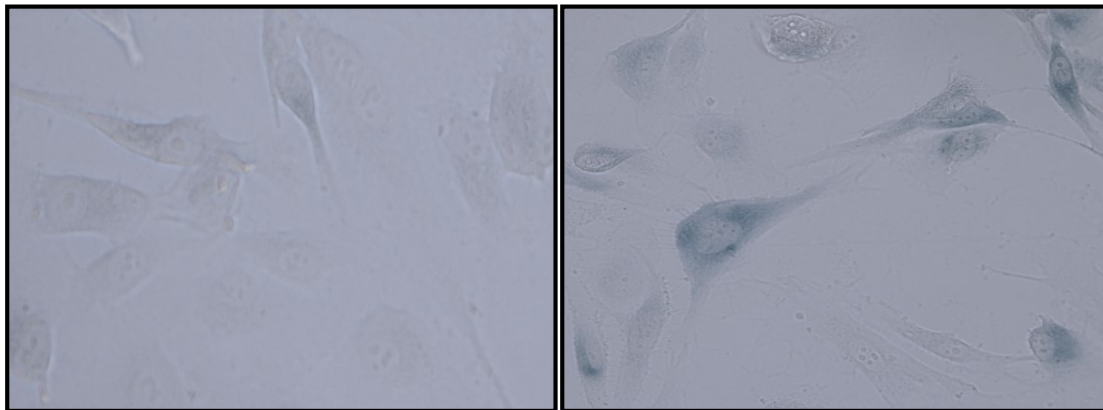


Figure 3 - Senescence-associated (SA)- β gal staining in HUVECs. Senescent cells show flattened structure

Representative pictures showing how images were processed for quantification of senescent cells. The right microscopy picture shows senescent cells and the left one presents non-senescent cells, which are smaller than senescent cells.

1.3.3 Senescence-associated β -D-galactosidase activity

The maximal activity of β -D-galactosidase in the lysosomes of non-senescent cells, which is encoded by the GLB1 gene, is at pH 4 (Lee et al, 2004). Lysosomal β -D-galactosidase is overexpressed in senescent cells, allowing x-gal staining at the suboptimal pH 6 to differentiate between normal and senescent cells (Figure 3). Thus β -D-galactosidase can be used as a reliable senescence biomarker (Dimri et al, 1995). The x-gal staining assay produces a blue perinuclear precipitate in β -D-galactosidase-positive cells (Christofalo et al, 1993) and therefore is a simple qualitative histochemical method to detect galactosidase at pH 6 in senescent cells, but not in presenescent or immortalized cells (Dimri et al, 1995). Fibroblasts from patients with autosomal recessive GM1-gangliosidosis, a lysosomal disorder in which galactosidase is defective, do not exhibit senescence-associated β -galactosidase

(SA- β -gal)staining when becoming senescent, demonstrating that β -galactosidase itself is not functionally required for senescence (Muller et al, 2009).

1.3.4 Altered gene expression and activation of tumor suppressor networks

Cells undergo senescence in response to a variety of signals, including shortened telomeres, DNA damage, oncogenes or supra physiological mitogenic signals. These cause irreversible changes in gene expression that regulate growth arrest and cellular senescence, including the p53, p21 and retinoblastoma (Rb) proteins (Dulic et al, 2000). Pathways that lead to cell cycle arrest are activated by stress factors such as the p38 mitogen-activated protein kinase (p38 MAPK). Key components of these senescence-regulating signaling pathways are discussed in more detail in later sections.

1.3.5 Chromatin architecture and senescence associated heterochromatin foci (SAHF)

Epigenetic gene regulation has been implicated in the process of senescence (Kiyono et al, 1998; Dickson et al, 2000). Global chromatin reorganization is not a specific senescence marker, but plays an important role in the senescence mechanism. High mobility group A (HMGA) proteins are senescence-associated chromatin binding proteins. Senescence-associated heterochromatin foci (SAHF) formation contributes to stable senescence arrest and causes the irreversibility of the senescent phenotype (Beausejour et al, 2003; Narita et al, 2003). Some senescence-inducing stimuli such as DNA damage and replicative stress induce HMGA upregulation (Narita, 2007). HMGA upregulation is an early event in response to oncogenic stimuli during tumorigenesis and activates the senescence program. HMGA1 is essential for SAHF architecture. SAHF are detectable through markers of heterochromatin, such as heterochromatin protein 1 (HP1), methylation (K3me3) of histone H3 (which creates a docking site for HP1) and exclusion of euchromatin markers, such as histone H3K9 acetylation and Lys4 tri-methylation (K4me3) (Narita, 2007). MacroH2A and histone chaperones asf1a and HIRA also play a critical role in SAHF formation (Zhang et al, 2005). MacroH2A is a transcriptionally repressive variant of histone H2A and is a marker of the inactive X (Xi) chromosome in female mammals, which is a form of facultative heterochromatin (Costanzi and Pehrson, 1998).

1.3.6 Autophagy

Autophagy is a catabolic process that is mediated by autophagosomes (membrane vesicles) that fuse with lysosomes. The cellular lysosomal degradation pathway involved in autophagy increases in activity with age (Dice, 1990) and is also a major component of the cellular stress response. Therefore, autophagy and senescence may be coupled responses that influence tumor growth and prolonged states of growth arrest. The stress of oncogene activation causes autophagy (Young et al, 2009). The activation of autophagy in senescent cells is correlated with down regulation of cell cycle exiting. Interestingly, autophagy related genes including ULK3, BNIP3 and BNIP3L are upregulated in senescent cells (Young et al, 2009).

1.4 Senescence induction

A variety of conditions can induce premature senescence. These include DNA-damage induced senescence, stress-induced senescence, oncogene-induced senescence (OIS), and tumor suppressor loss-induced senescence.

1.4.1 DNA-damage induced senescence

Reactive oxygen species (ROS), ionizing radiation and ultraviolet light can induce oxidation of DNA bases and generate single-strand (SSB) or double-strand breaks (DSBs) (Hoeijmakers, 2009). Chemical agents used in cancer chemotherapy can cause a variety of DNA lesions. Alkylating agents such as methyl methanesulfonate and temozolomide attach alkyl groups to DNA bases, which introduce covalent links between bases of the same DNA strand (intrastrand crosslinks) or between different DNA strands (interstrand crosslinks) (Iyer & Szybalski, 1964). Many repair mechanisms counteract DNA damage. Mismatched DNA bases are replaced with correct bases by mismatch repair. Small chemical alterations of DNA bases are repaired by base excision repair (Jiricny, 2006; Lindahl, 2000). Pyrimidine dimers and intrastrand crosslinks are corrected by nucleotide excision repair through the removal of an oligonucleotide of 30bp containing the damaged bases (Moldovan, 2009). SSBs are repaired by single-strand break repair and DSBs are processed either by nonhomologous end joining or homologous recombination (Caldecott, 2008).

In response to DSBs, the ATM protein is activated via phosphorylation on multiple residues (Bakkenist, 2003), and ATR in complex with its partner protein (ATRIP) is

activated in DSBs (Cimprich, 2008). ATM and ATR are required for all repair mechanisms, including non-homologous end joining, homologous recombination, and interstrand crosslinks repair. Both proteins phosphorylate and activate p53 (Giaccia, 1998). This activation of p53 leads to the senescence that can ensue following DNA damage (Canman et al, 1994).

1.4.2 Stress- induced senescence

In vitro, abnormal concentrations of nutrients and growth factors, the presence of O₂ above physiological levels, and other sources of oxidative stress (e.g. H₂O₂ and tert-butylhydroperoxide), as well as other stressors such as ethanol, ionizing radiation and mitomycin, or the absence of extracellular matrix components, can induce premature senescence (Sherr and Depinho, 2000). Higher levels of stress generally result in apoptosis, while senescence is induced in response to lower levels of stress. This type of senescence is independent of telomere length (Prowse and Greider, 1995).

1.4.3 Oncogene-induced senescence (OIS)

Oncogenes such as Ras (Serrano et al, 1997) or Raf (Zhu et al, 1998) can induce differentiation, apoptosis or senescence in normal human cells, which is called oncogene-induced senescence (O'shae et al, 1996; Kaufman et al, 1997). Oncogenic Ras is mitogenic, and activates the Raf-MEK-ERK signaling cascade. Constitutive mitogenic signals trigger Ras-induced cell cycle arrest through accumulation of p16, p19, p21 and p53 (Lin et al, 1998; Palmero et al, 1998). Activated (mutant) oncogenes such as H-Ras^{V12} induce cell cycle arrest and OIS (Land et al, 1983; Franza et al, 1986; Serrano et al, 1997) in a p53-dependent manner. In the absence of p53, Ras/Raf signaling induces transformation rather than senescence (Kemp et al, 1993; Lin et al, 1998). Raf-induced senescence is irreversible. The signal from Raf that induces senescence is transmitted through MEK. Thus OIS can be inhibited by blocking MEK using pharmacological drugs (Zhu et al, 1998).

1.4.4 Tumor suppressor loss-induced senescence in vitro

Loss of tumor suppressors such as PTEN (a phosphatase that counteracts pro-proliferative, pro survival kinases) (Alimonti et al, 2002) and NF1 (the gene responsible for the familial cancer syndrome neurofibromatosis type 1 (Courtois-Cox

et al, 2006) can cause senescence in mouse and human cells. For example, the loss of PTEN in MEF cells leads to senescence induction (Chen et al, 2005). Depletion of NF1, which encodes a RasGAP protein, leads to activation of Ras and thereby to induction of senescence (Basu et al, 1992).

1.5 Regulation senescence by signal transduction pathways

As described in Section 1.4, a variety of stresses are able to induce senescence. Many of the intracellular signaling pathways thereby activated mediate their activity through p53 (Figure 4), for example by increasing its transcription, its stability, and/or through modifying its phosphorylation or acetylation (Qian and Chen, 2013).

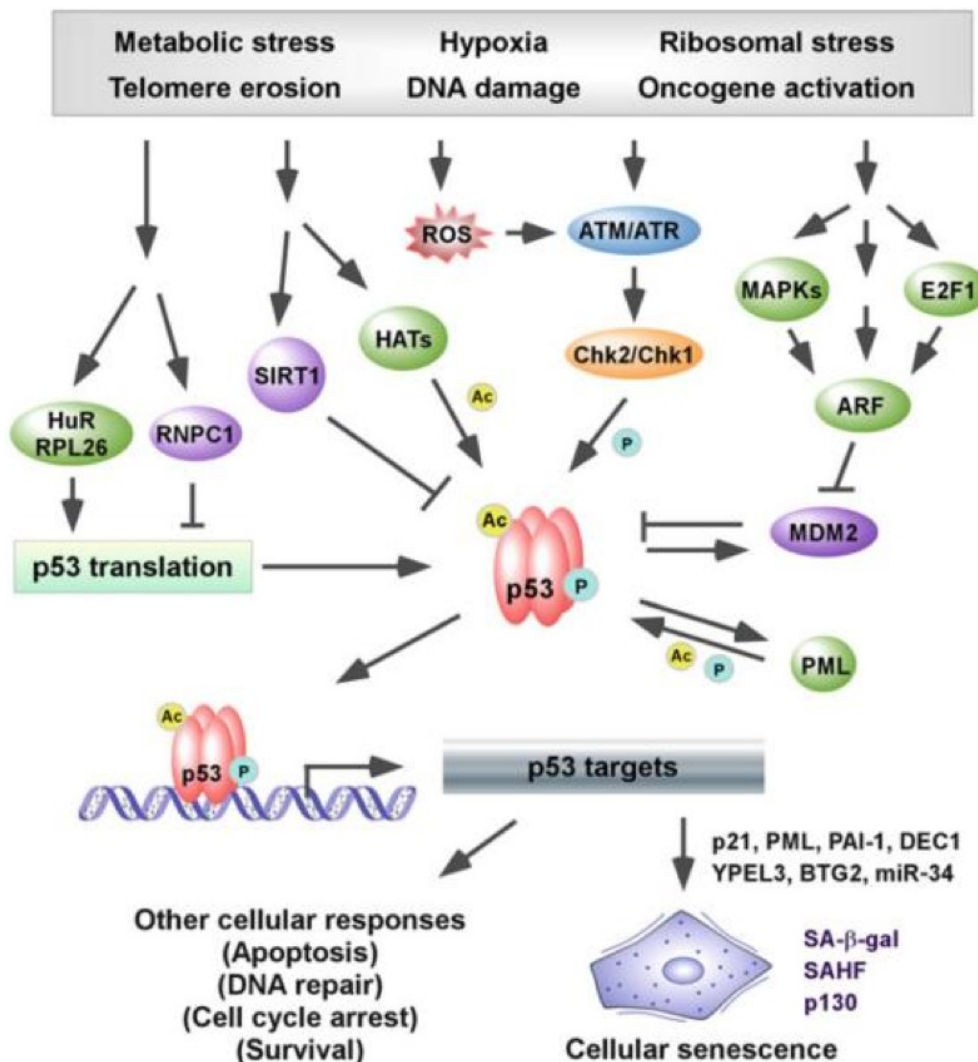


Figure 4 - The role of p53 in cellular senescence

Stress factors induce senescence through deregulated expression of p53 targets. A number of modifications of p53 contribute to this deregulation, including phosphorylation (through ATM/ATR-

Chk2/Chk1), acetylation (through p300/CBP, PCAF, Tip60/hMOF, and SIRT1), increased protein stability (through ARF-MDM2), and increased translation rates (through RNP1, HuR, and RPL26). PML regulates p53 stability by positively modulating its acetylation and phosphorylation levels. Some p53 target genes including p21, PML, PAI-1 and DEC1 functionally promote cellular senescence, and cause the typical senescence phenotype that is associated with hyperphosphorylation of p130 (Qian and Chen, 2013).

During the induction of replicative senescence, activation of ATM or ATR leads to upregulation or phosphorylative activation of p53 and thus senescence (Herbig et al, 2004). In OIS, oncogenic Ras induces senescence in cells with wild-type p53, but transforms cells lacking p53 (Kemp et al, 1993; Serrano et al, 1997), again underscoring the role of p53 in the induction of senescence. Although not true for all genotoxic stressors, p53 is required for senescence induced by chemotherapeutic drugs such as camptothecin, doxorubicin and cisplatin (Ewald et al, 2010).

Activation of p53 induces the expression of p21^{WAF1}, and/or increases the expression of p16^{INK4A} (Serrano et al, 1997). Both p21^{WAF1} and p16^{INK4A} are inhibitors of cyclin-dependent protein kinases (CDKs) that phosphorylate and inactivate the retinoblastoma protein (Rb). Subsequent accumulation of the hypophosphorylated, active form of Rb leads to cell-cycle arrest and other phenotypes associated with senescence (Xu et al, 2014).

Several signal transduction pathways can trigger senescence (Figure 5). For example, mitogen-activated protein kinases (MAPKs) play important roles in senescence induction. In particular, the JNK and p38 MAPK pathways are activated by cytotoxic stresses including UV irradiation, chemotherapy, heat shock and inflammatory cytokines (Zanke et al, 1996). During OIS, sequential activation of the Raf–MEK–ERK and MKK3/6–p38 pathways results in activation of three p38 isoforms, p38 α , p38 γ , and p38 δ that induce senescence in a coordinate manner (Xu et al, 2014). p38 α induces transcription of p16^{INK4A}. Both p38 α and p38 γ stimulate the activity of p53 by phosphorylation. Once activated, p53 induces the expression of p21^{WAF1}, which, together with p16^{INK4A}, triggers senescence. On the other hand, p38 δ mediates senescence independently of p53 and p16^{INK4A}, for example through regulating the activity of the DNA-damage checkpoint kinases CHK1 and CHK2.

The PI3K/AKT/mTOR pathway also plays a role in the induction of senescence, for example during ras-induced OIS or tumor suppressor loss-induced senescence. In the latter example, loss of PTEN leads to activation of the PI3K/AKT/mTOR pathway. In turn, activated mTOR stimulates the translation of p53, leading to p21^{WAF1} expression and induction of senescence (Xu et al, 2014, Figure 5).

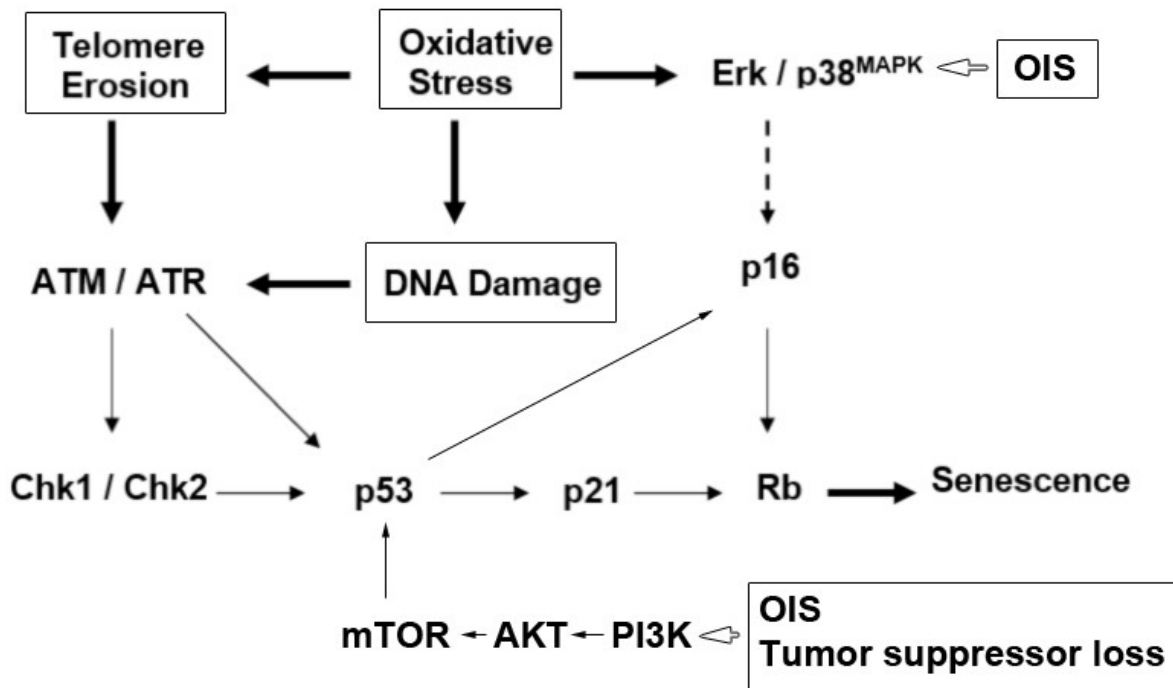


Figure 5 - Pathways to senescence

Summary diagram showing some of the pathways activated by various stimuli that lead to senescence (modified from Muller et al, 2008). See text for details.

Despite the evidence implicating p53 in the induction of senescence, in some contexts p53 has also been shown to suppress senescence (reviewed in Vigneron and Vosden, 2010) for example in human fibroblasts that lose both wild-type p53 alleles (Medcalf et al, 1996) or express a dominant negative p53 allele (Medcalf et al, 1996; Bond et al, 1994). Notably, p53 can suppress senescence while promoting cell cycle arrest (Demidenko, 2010).

The paradoxical ability of p53 to both suppress and induce senescence is likely due in part to the ability of p53 to both positively and negatively regulate oxidative stress. On one hand, p53 can increase levels of ROS (Reactive Oxygen Species) that play an important role in senescence (Johnson et al, 1994). On the other hand p53

induces antioxidant pathways (Olovnikov et al, 2009). The balance between suppression and induction of senescence by p53 is thought to involve mTOR. As pointed out above, mTOR signaling promotes senescence. However, p53 inhibits mTOR, which contributes to the anti-senescence effect of p53 (Feng and Levine, 2010; Korotchkina et al, 2010). On the other hand, increased ROS levels – as induced by p53 – activate mTOR (Blagosklonny, 2008, Figure 6).

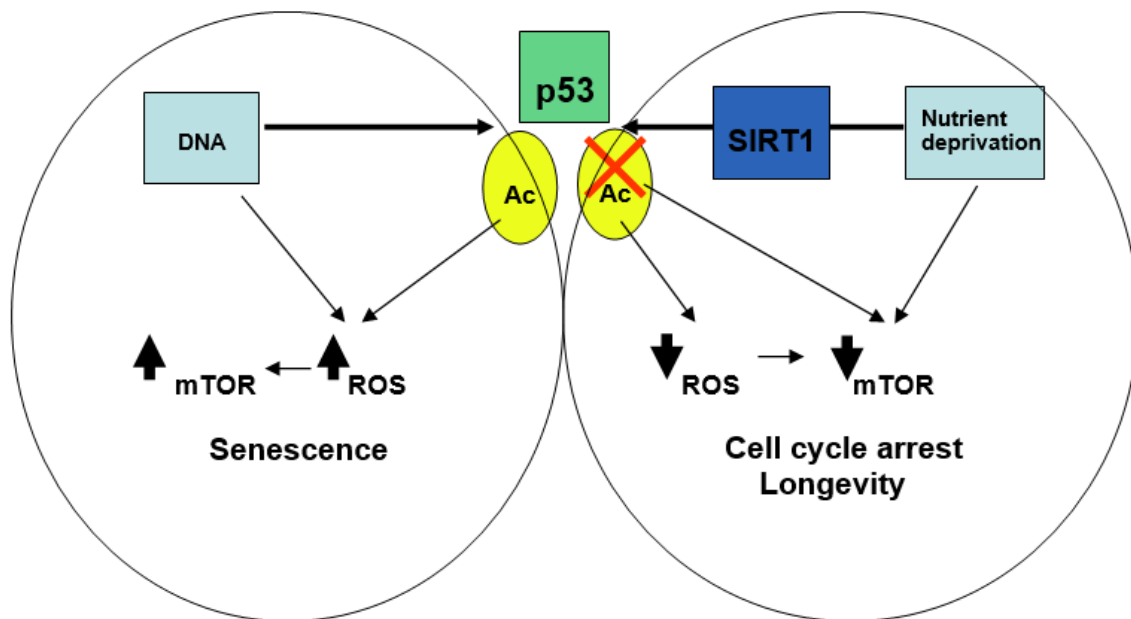


Figure 6 - Schematic representation of p53 acetylation, mTOR activity and the induction of senescence or cell cycle arrest

Oxidative stress induces senescence by deacetylation of p53, which promotes the activity of mTOR. SIRT1 activity under nutrient deprivation deacetylates p53, thus inhibits mTOR activity, which leads to increased longevity (modified from Vigneron et al, 2010).

1.6 SIRT1 and senescence

SIRT1 is a NAD⁺-dependent deacetylase localized in the nucleus that belongs to the sirtuin family, and deacetylates acetyl-lysine residues on various proteins. SIRT1 was first identified in yeast as a transcriptional regulator with the name of silent information regulator 2 (Sir2). The upregulation of Sir2 leads to an extension in the life span of *Saccharomyces cerevisiae* (Tissenbaum and Guarente, 2001) and *Caenorhabditis elegans* in response to caloric restriction (Wood et al, 2004). Therefore, SIRT1 might also regulate life span in mammals (Bordone et al, 2006). SIRT1 expression is strongly downregulated in senescent cells (Sasaki et al, 2006). Accordingly, SIRT1 blocks endothelial cell senescence (Huffman et al, 2007; Chu et

al, 2005). Sirtinol, an inhibitor of SIRT1, induces senescence in breast and lung cancer cells (Liu et al, 2006). Hyperforin also has an inhibitory effect on SIRT1 (Gey et al, 2007), supporting the notion that hyperforin may induce senescence.

Mechanistically, SIRT1 physically interacts with p53 and deacetylates p53 at its C-terminal Lys382 residue (Vaziri et al, 2001). As acetylation of p53 promotes senescence (Sakaguchi et al, 1998), this provides a mechanism whereby SIRT1 may inhibit p53-induced senescence. Thus if SIRT1 is inactivated by sirtinol, p53 remains acetylated and is thereby able to induce senescence (Grozing et al, 2001). A similar mechanism of action is conceivable for hyperforin, as hyperforin inhibits SIRT1 (Gey et al, 2007). SIRT1 is also able to deacetylate a number of transcription factors including FOXO1, FOXO3, FOXO4, Ku70, NFkB and MyoD (Gey et al, 2007), thereby regulating their activity. Resveratrol (RSV), a polyphenol found in red wine, stimulates the deacetylase activity of SIRT1 (Howitz et al, 2003).

In chronic lymphatic leukemia cells, hyperforin upregulates Noxa, a primary p53 response gene and proapoptotic protein (Zaher et al, 2009). Noxa belongs to the BH3-only group of the BCL2 family, which does not activate Bax/Bak (proapoptotic proteins) directly, but neutralizes prosurvival proteins (Delia et al, 1995). At least eight BH3-only members have been identified, including Bad, Bid, Bik, Bim, Bmf, Hrk, Noxa and Puma.

Noxa mRNA is rapidly induced after adenovirus-mediated introduction of p53 into fibroblasts derived from p53^{-/-} or wild type mice. Promoter analysis of the human Noxa gene revealed the presence of a *bona fide* p53 response element 195bp upstream of the transcriptional start site (Oda et al, 2000). The oncogene Ras induces both senescence and Noxa expression (Nicke et al, 2005). Noxa expression may therefore conceivably play a role in senescence, providing a further link between hyperforin and the induction of senescence.

1.7 Analysis of senescent cells

The analysis of senescent cells requires a reproducible assay to differentiate senescent from dividing or apoptotic cells. Most commonly, 5-bromo-4-chloro-3-indolyl β -D-galactoside (x-gal) is used for senescence detection. As outlined above, x-gal staining can be used to identify senescent cells because β -galactosidase is

overexpressed in senescent cells (so-called senescence-associated β -galactosidase (SA- β -gal), and therefore its activity can be detected at pH 6, which is suboptimal for enzymatic activity, meaning that the lower levels of β -galactosidase in non-senescent cells are not detectable. When x-gal is cleaved, an intense blue halogenated indoxyl (C_8H_7NO) derivative is formed (Dimri et al, 1994), allowing the percentage of positively stained cells to be counted under the microscope. Due to the fact that manual counting is very time consuming, part of my thesis was devoted to the development of methods for the analysis of senescent cells more rapidly and more precisely by using specific fluorescence markers of senescent cells such as 5-dodecanoyl-aminofluorescein di- β -D galactopyranoside ($C_{12}FDG$), LysoTracker yellow and 4-methylumbelliferone, to allow the quantification of senescent cells more rapidly and sensitively.

The β -galactosidase substrate $C_{12}FDG$ has been used to develop a highly sensitive flow cytometric β -galactosidase assay in live mammalian cells (Noppe et al, 2009). $C_{12}FDG$ is a membrane permeable, non-fluorescent substrate of β -galactosidase. After hydrolysis, the glycosyl residues emit green fluorescence and the hydrolysed compound remains confined within the cell, as it becomes membrane insoluble (Kurz et al, 2000). I aimed to develop a flow cytometry-based technique to quantify SA- β gal activity using $C_{12}FDG$ in conjunction with flow cytometry, which compared with the cytochemical method would not be subjective and has a higher throughput (Kurz et al, 2000).

2 AIMS OF MY STUDY

Previous studies have shown that hyperforin can induce apoptosis above certain threshold concentrations, but below these concentrations can nevertheless inhibit proliferation by inducing cell cycle arrest in the absence of apoptosis induction. Circumstantial evidence suggests that hyperforin can activate signaling pathways associated with the induction of senescence. The aim of my study was therefore to determine whether hyperforin induces senescence in tumor cells and endothelial cells at non-apoptosis-inducing concentrations, both in cell culture and in vivo. If so, I then planned to study the molecular mechanism by which hyperforin induces senescence. Finally I aimed to establish improved methods for the analysis of senescent cells.

The specific aims of my study were as follows:

- Determine whether hyperforin induces senescence in tumor cells and ECs using x-gal staining, and investigate the concentration and time-dependency of any effects observed
- Treat tumor-bearing animals with hyperforin in vivo to determine whether it is also able to induce senescence in vivo
- Study the molecular pathway through which hyperforin induces senescence, focusing on SIRT1, p53 and Noxa.
- Establish methods to quantify senescent cells more quickly and specifically than standard x-gal staining methods.

3 MATERIAL AND METHODS

3.1 Materials

3.1.1 Instruments

Centrifuges	Thermo Fisher Scientific, Schwerte
Developer for X-ray films	CAWOMAT 2000R CAWO, Schrobenhausen
Electrophoresis Apparatus	PeqLab, Erlangen; BioRad, München
ELISA reader Multiskan Acscent	Thermo Fisher Scientific, Schwerte
FACS-can	BectonDickinson, Franklin Lakes USA
Fluorescence microscope Axio Imager	Carl Zeiss, Jena
Incubator Binder	Tuttlingen
Incubator HeraCell	Thermo Fisher Scientific, Schwerte
Microscope Axiovert 40 CFL	Carl Zeiss, Jena
NanoDrop	PeqLab, Erlangen
Shaker for bacteria Certomat IS	Sartorius, Göttingen
Sonicator Sonoplus	Bandelin, Berlin
Sterile hood Hera Safe	Thermo Fisher Scientific, Schwerte
Thermomixer 5436	Eppendorf, Hamburg
Ultracentrifuge Sorval RC6plus	Thermo Fisher Scientific, Schwerte
Vortex	VWR International, UK

Water bath

Memmert, Büchenbach

3.1.2 Chemicals, reagents and consumables

0.25% Trypsin-EDTA (1x), phenol red

Life Technologies, Darmstadt

AceGlow

PeqLab, Erlangen

Acetic acid

Roth, Karlsruhe

Acrylamide/N,N'-Methylenbisacrylamide
(37,5:1)

Roth, Karlsruhe

Agarose

Biozym, Wien, Austria

Ammonium peroxodisulfate (APS)

Roth, Karlsruhe

Ampicillin

Roth, Karlsruhe

Aristoforin

Prof. Giannis, University of Leipzig

Bafilomycin A1

Sigma Aldrich, Steinheim

BCA assay

Thermo Fisher Scientific, Schwerte

Bovine serum albumin (BSA)

PAA, Pasching, Austria

Bromophenol blue

Roth, Karlsruhe

Butanol

Roth, Karlsruhe

Cell death detection ELISA

Roche, Mannheim

C₁₂FDG

Invitrogen

CHAPS

Fulka, Switzerland

Chloroform

Roth, Karlsruhe

Coomassie Brilliant Blue R250	Roth, Karlsruhe
Diethylpyrocarbonate (DEPC)	Roth, Karlsruhe
Dimethylsulfoxide (DMSO)	Sigma Aldrich, Steinheim
Dithiothreitol (DTT)	Fluka, Neu-Ulm
Dulbecco's modified Eagle Medium (DMEM)	Life Technologies, Darmstadt
ECL-Western blotting detection reagent	Thermo Fisher Scientific, Schwerte
Ethidium bromide	Roth, Karlsruhe
Ethylenediaminetetraacetic acid (EDTA)	Sigma Aldrich, Steinheim
Fetal Calf Serum (FCS)	Life Technologies, Darmstadt
Formaldehyde	Roth, Karlsruhe
Glutaldehyde	Roth, Karlsruhe
Glycerol	Sigma Aldrich, Steinheim
Glycine	Roth, Karlsruhe
HEPES	Roth, Karlsruhe
Hyperforin	Prof. Giannis Lab, University of Leipzig
Lipofectamine 2000	Life Technologies, Darmstadt
Lipofectamine LTX	Life Technologies, Darmstadt
Lysotracker yellow	Invitrogen
Magnesium chloride	Roth, Karlsruhe
Methanol	Roth, Karlsruhe

Milk powder	Sigma Aldrich, Steinheim
4-methylumbelliferyl- β -D-galactopyranoside (MUG)	Sigma Aldrich, Steinheim
N,N,N',N'-Tetramethylethylenediamine (TEMED)	Roth, Karlsruhe
Oligonucleotides	Metabion
OptimMem	Life Technologies, Darmstadt
Paraformaldehyde	J.T. Baker, Deventer, The Netherlands
Penicillin/Streptomycin	Life Technologies, Darmstadt
Phenol	Roth, Karlsruhe
Phenylmethylsulfonyl fluoride (PMSF)	Roth, Karlsruhe
Phosphate buffer saline (PBS)	Life Technologies, Darmstadt
Plasmid Maxi Kit	Qiagen, München
Propanol	Roth, Karlsruhe
Reagents for developer	AGFA, Bonn
Restriction enzymes and buffers	Fermentas
Resveratrol	Sigma Aldrich, Steinheim
Sirtinol	Sigma Aldrich, Steinheim
SOC	Life Technologies, Darmstadt
Sodium acetate	Roth, Karlsruhe
Sodium chloride	Roth, Karlsruhe
Sodium orthovanadate	Roth, Karlsruhe

Sodium dodecylsulfate (SDS)	Roth, Karlsruhe
Sodium hydroxide (NaOH)	Roth, Karlsruhe
Tip-500-columns	Qiagen, München
Tris-HCl, Tris-Base	Sigma Aldrich, Steinheim
Triton X-100	Sigma Aldrich, Steinheim
Trizol	Life Technologies, Darmstadt
Tryptone	Roth, Karlsruhe
Tween 20	GE Healthcare, München
X-gal	Sigma Aldrich, Steinheim
Yeast extract	Roth, Karlsruhe

3.1.3 Antibodies

3.1.3.1 Primary antibodies

Anti- β -actin	mouse, monoclonal, Sigma
Anti-Noxa	mouse, monoclonal, US Biological
Anti-SIRT1	rabbit, polyclonal, Abcam
Anti-H4	mouse, monoclonal, Sigma
Anti-H4Ac	rabbit, polyclonal, Abcam

3.1.4 Secondary antibodies

All secondary antibodies were from DAKO, polyclonal, produced in goat:

Anti mouse HRP

Anti rabbit HRP

Anti Rat HRP

3.1.5 Cells

Eukaryotic cells:

NAME	SPECIFICATION	REFERENCE	SOURCE
HUVEC	Human umbilical vein endothelial cells	(Jaff EA et al, 1973)	Promocell
LEC	Human lymphatic endothelial cells	(Casley-Smith, 1961)	Promocell
MCF-7	Human breast adenocarcinoma	(Rockville et al, 1985)	ATCC
T47D	Human breast adenocarcinoma	(Rockville et al, 1985)	ATCC
HCT116	Human colon carcinoma	(Dexter et al, 1979)	ATCC
HCT+/, HCT-/-	Human colon carcinoma	(Bunz et al, 1999)	Dr. Blattner , ITG Karlsruhe
ACC57	Human cervix carcinoma	(Akiyama et al, 1985)	ATCC
PC3	Human prostate carcinoma	(Nagafuchi, 1989)	ATCC
SW480	Human colon carcinoma	(Goyette et al, 1992)	ATCC

3.1.6 Buffers and solutions

All solutions were prepared with double deionized water (ddH₂O).

Buffer	Composition
5x TBE buffer	400 mM Tris, pH 8.0 EDTA 10 mM EDTA Acetic acid for pH titration
6x DNA loading buffer	0.25% (w/v) Bromphenol blue 0.25% (w/v) Xylene cyanol FF 40% (w/v) sucrose
6x Laemmli sample buffer	350 mM Tris, pH 6.8 30% glycerin 1% SDS 0.5 M DTT 12% Bromophenol blue
LB-agar (autoclaved)	1.5% (w/v) Bacto agar in LB medium
LB-medium (autoclaved)	1% (w/v) Bacto tryptone 0.5% (w/v) Bacto yeast extract 170 mM NaCl adjusted to pH 7.6 with NaOH
RIPA buffer	150 mM NaCl 0.1% Nonidet P40 0.5% Sodium deoxycholate

	0.1% SDS
	50 mM Tris pH 7.0
	1 mM EDTA
4X Loading Buffer	0.1 M Tris-HCl pH 6.8
	8% SDS
	40% glycerol
	0.02% Bromophenol Blue
	0.1 M DTT
1x Running buffer	25 mM glycine
	192 mM Tris
	0.1% SDS
Staining solution	2% Coomassie brilliant blue
	40% methanol
	5% glacial acetic acid
	Water up to volume
De-staining solution	40% methanol
	5% glacial acetic acid
	Water up to volume
1x Transfer buffer	25 mM glycine
	192 mM Tris
	0.1% SDS

	Methanol 15%-20% according to protein size
Tris-buffered saline (TBS) 10X	500 mM Tris HCl, pH 7.4 1.5 M NaCl
Washing buffer	1X TBS 0.05% Tween
Blocking buffer	1% Bovine serum albumin 1X TBS 0.05% Tween
Stripping solution	2% SDS 0.7% β -mercaptoethanol 62.5 μ M Tris-HCl pH 6.8
X-gal buffer	1 mg/ml x-gal 0.12 mM $K_3Fe[CN]_6$ 0.12 mM $K_4Fe[CN]_6$ 1 mM $MgCl_2$ adjusted to pH 6.0 with PBS

3.2 Methods

3.2.1 DNA Quantification

To quantify the amount of DNA, the optical density (O.D.) at 260, 280 and 230 nm was measured with a NanoDrop® device and ND-1000 software (version 3.1.2). An $OD_{260}=1$ corresponds to 50 µg/ml of double-stranded DNA. An OD_{260}/OD_{280} ratio of 1.8 indicates a nucleic acid preparation relatively free from protein contamination. An OD_{260}/OD_{230} ratio above 1.6 indicates a preparation free of organic chemicals and solvents.

DNA concentration (µg/ml) = $(OD_{260}) \times (\text{dilution factor}) \times (50 \text{ µg DNA/ml}) / (1 \text{ } OD_{260} \text{ unit})$

3.2.2 Agarose gel electrophoresis

The agarose was dissolved in 1xTAE buffer. The mass of the agarose was dependent on the size of the fragments to be analyzed (0.8-1.5%). After cooling, ethidium bromide (EtBr) solution (0.5 mg/ml final concentration) was added to the liquid agarose. The liquid agarose with EtBr was poured into the running chamber with a comb. The comb was removed and the chamber was filled with 1xTAE buffer. The DNA was loaded into the wells and separated electrophoretically. The bands were detectable at 265 nm.

3.2.3 Preparation of $CaCl_2$ competent E. coli cells

LB medium (50 ml) containing selection antibiotics was inoculated with a bacterial culture at OD_{600} of 0.06. During the logarithmic phase of the bacterial growth, cultures were centrifuged at 4,000 rpm for 10 minutes at 4°C. The resulting pellet was first washed in 20 ml 0.1 M $MgCl_2$ and then centrifuged as before. The pellet was then resuspended in 20 ml 0.1 M $CaCl_2$ and centrifuged again, then resuspended in 2 ml 0.1 M $CaCl_2$, and incubated on ice for a minimum of 2 hours. Finally, sterile glycerol (ratio 1:1) was added and the aliquoted competent cells were frozen in liquid nitrogen.

3.2.4 Transformation of competent E. coli cells

Calcium chloride weakens the capsular structure of E. coli cells, allowing the transfer of plasmids into bacteria by a short heat pulse (Dagert and Ehrlich, 1979). For bacterial transformation 10 µl ligation mixture was combined with 100 µl of

CaCl₂competent bacterial suspension, incubated on ice for 15 minutes, and then heat-shocked at 42°C for 90 sec. After 3 minutes incubation on ice, 200 µl LB medium was added to each tube and cells were placed on a shaker for 45 minutes at 37°C. Transformed *E. coli* cells were then plated out on agar dishes containing an antibiotic, resistance against which was conferred by the vector used for transformation. Therefore, only bacteria carrying the incorporated plasmid were able to grow.

3.2.5 Isolation of plasmid DNA from *E. coli* cells

For evaluation of cloning results, a small-scale plasmid preparation (“miniprep”) was used. For this purpose, several bacterial colonies were picked from an agar plate, and each was used to inoculate 5 ml of LB medium containing the appropriate selective antibiotic. After an overnight incubation at 37°C, bacterial plasmids were purified using QIAprep Spin Miniprep Plasmid Purification Kit (QIAGEN) according to the manufacturer’s instructions. Briefly, an overnight culture of *E. coli* was harvested by centrifugation (4.500 rpm, 10 minutes, 4°C), and the pellets were resuspended in 250 µl buffer P1 containing 100 µl/ml RNase A. An equal amount of the lysis buffer P2 was added, and gently mixed by inverting the tube 10-15 times. After a maximum lysis time of 5 minutes at RT, 350 µl of neutralizing buffer P3 was mixed with the contents of the tube, and the resulting cell debris, cellular proteins and chromosomal DNA were pelleted by centrifugation (13.000 rpm, 10 minutes, RT). The supernatant containing the dissolved plasmid DNA was then transferred to a spin column, left for 1 minute to equilibrate, and centrifuged (13.000 rpm, 1 minute, RT). The flow-through was discarded, and the column was washed with 750 µl wash buffer. After removal of the wash flow-through, the column was spun dry and placed on a fresh reaction tube. Then, 30-50 µl double distilled H₂O was applied to the column, and the DNA was eluted by a final centrifugation step (1 minute, 13.000 rpm, RT).

For a larger preparation of plasmid DNA (maxiprep), 200 ml of LB medium was inoculated with a bacterial culture and purified with the QIAfilter Plasmid Maxi Kit (QIAGEN) according to the manufacturer’s instructions. After extraction of plasmid DNA by mini- or maxiprep, its absorbance at 260 nm was measured. As already briefly described in 3.2.2, an OD₂₆₀ value of 1 unit corresponds to a

concentration of 50µg/ml of double-stranded DNA. After quantification all purified DNA was diluted as appropriate and stored at -20°C.

3.2.6 Cell culture methods

Cryopreserved tumor and endothelial cells were removed from liquid nitrogen and thawed for 1-2 min with constant agitation to quickly thaw the cells. Slowly, drop-by-drop, cells were diluted in a 10-fold volume of pre-warmed growth medium in a culture dish. The cells were incubated at 37°C in an incubator (Hera Cell 150) with 5% CO₂ and 95% air humidity, except for LECs which were kept for a maximum of 6 passages under the same conditions as the other cells, but with 3% O₂. In general, cells were allowed to grow until a confluency of 80-90% was reached. The cell monolayer was washed with PBS and trypsin /EDTA (1 ml per 25 cm² of surface area) was added to the washed cell monolayer. The flask was returned to the incubator and incubated for 1-2 min or until cells were detached. Fresh medium was added and the cells were replated at the desired density. All cell lines were routinely screened for mycoplasma using VectorGem Myco Detection Kit (Vector). Only early passage primary endothelial cell cultures were used for all experiments.

Treatments of cells with hyperforin, aristoforin, RSV and sirtinol: 0.25 mg hyperforin or aristoforin were dissolved in 23 or 21 µl DMSO, respectively, which corresponds to 20 mM of each of the agents. To obtain the desired final concentrations, the 20 mM hyperforin or aristoforin stock solutions were diluted in the medium and the cells were treated immediately. A concentration of 70 mM RSV correlates to 16 mg RSV dissolved in 1 ml DMSO. A 1 mM solution of sirtinol was obtained by dissolving 1 mg sirtinol in 2.5 ml DMSO. As different end concentrations of DMSO were used in the experiments, appropriate DMSO controls were added for each treatment in all experiments. In experiments in which the cells were treated every two days for 6 days, medium was removed every 48 h and the cells were treated with fresh medium for the next 48 h.

Freezing protocol: Logarithmically growing cells were trypsinized, harvested by medium addition and centrifuged as described above. The supernatant was then removed and the cells resuspended in normal culture medium containing 10% DMSO. The suspension was placed in 1.8 ml freezing vials. Prepared cells were immediately placed in - 80°C and after some days moved to liquid nitrogen.

3.2.7 DNA plasmid transfection of cultured cells

When cells reached a density of 80-90% confluency, the culture medium was removed and replaced with serum-free Opti-MEM medium. For a 6-well plate, Lipofectamine 2000 was added to 250 μ l Opti-MEM in 1.5 ml microfuge tube and incubated for 5 min at RT. DNA (2 μ g in 250 μ l Opti-MEM) and the diluted lipofectamine 2000 were then combined and incubated for 20 min at RT. DNA and lipofectamine 2000 mixture was subsequently added to the cells. The medium was replaced after 6 h with the fresh culture medium.

3.2.8 RNA interference

For all siRNA oligonucleotides, the transfection was performed as follows. Cells were seeded to reach a confluency of ~50% on the transfection day. Both the oligonucleotides and the Lipofectamine 2000 were separately diluted in OptiMem according to the Lipofectamine 2000 protocol. The ratio nmol siRNA: μ l Lipofectamine 2000 was always 0.1:5. In case of a co-transfection, the RNA amount was divided equally between the two sequences, in order to maintain a constant total amount of RNA. Briefly, the diluted Lipofectamine 2000 was incubated for five minutes at RT, and subsequently combined with the diluted oligonucleotides. The mixture was incubated for 20 minutes at RT, and finally added dropwise to the cells. These were maintained in medium containing FCS, but without antibiotics. The knock down was most efficient after 72 hours for all three siRNAs. Scrambled controls were used for each siRNA.

3.2.9 Preparation of cell lysates

Cells were harvested and counted. To lyse the cells, 100 μ l ice-cold lysis buffer (RIPA buffer) was added for every 1×10^6 cells. The lysate was incubated on ice for 30 min, then transferred into a microcentrifuge tube and centrifuged at 14,000 rpm for 15 min at 4°C. The protein concentration in the soluble supernatant was determined using the Bradford protein assay. The soluble supernatant was then diluted in 2x sample buffer and boiled for 5 min at 95°C. Aliquots were stored at -20°C or -80°C.

3.2.10 Protein concentration determination

The protein concentration of cell lysates was assessed with a commercially available bicinchoninic acid assay, using known concentrations of bovine serum

albumin for the calibration curve. A 1:5 dilution of the lysate was used for the colorimetric reaction that was performed in flat bottom 96 well plates. The color development is proportional to the amount of protein present in the solution, and was measured at 595nm with an ELISA reader. The concentration was then calculated with the Ascent software, according to the calibration curve.

3.2.11 SDS-PAGE and Western Blotting

The samples were added to 6x sample buffer containing 100mM DTT. Heating for 5 minutes at 95 °C denatured the samples and then tubes were spun at 13,000 rpm for ~1 min. SDS polyacrylamide gel electrophoresis (SDS-PAGE) was performed as described by Laemmli (Laemmli, 1970). Depending on the molecular mass of the protein of interest, 8 to 15% polyacrylamide gels were used. The protein samples were loaded onto the gel and the gel was run at about 60 V until the dye migrated through the stacking gel, then the voltage was increased to about 85 V until the dye front reached the bottom of the separating gel. Gels were western blotted onto a nitrocellulose membrane. The gel and membrane were sandwiched between a sponge and Whatman paper. The gel was placed on the side of the negative electrode in the transfer apparatus. Electrotransfer was performed at 27 V for 12h. After transfer, the membrane was incubated in blocking buffer (5% nonfat dry milk in TBST) for 1 h at RT. The protein of interest was detected with a primary antibody solution at 4°C overnight. The membrane was washed three times for 5 min in 1x TBST buffer at RT, then incubated with a secondary antibody for 1 h at RT, and was then washed again with TBST. The proteins were detected using the Western Lightning chemiluminescence kit.

3.2.12 FACS analysis

Cells were suspended in 70 µl of PBS/ 10% FCS, then incubated with primary antibodies directed against the protein of interest for one hour at 4°C. The cells were washed twice, then resuspended in 100 µl PBS/ 10% FCS containing appropriate secondary antibodies, and incubated for 30 minutes at 4°C. After washing three times with 150 µl PBS, the cells were resuspended in PBS/ 10% FCS and analysed with a FACScan cytometer (Becton Dickinson). The ideal concentration of both primary and secondary antibodies was determined in titration experiments. All the

FACScan operations performed in this study were done under the kind supervision and help of Melanie Grassl (if performed in the CBTM - Mannheim).

3.2.13 Senescence-associated- β -gal staining

Monolayers of cells were washed twice with PBS pH 6.0, and then fixed with 0.2% glutaraldehyde prepared in PBS pH 7.5 for 10 min. The cells were then washed twice again with PBS pH 6.0 containing 1mM MgCl_2 . After the last wash, staining solution was added [1 mg/ml 5-bromo-4-chloro-3-inolyl- β -D-galactosidase (x-gal)] in dimethylformamide (20mg/ml stock), 0.12 mM potassium ferrocyanide, 0.12 mM potassium ferricyanide, 1mM MgCl_2 in PBS pH 6.0 and the cells were incubated at 37°C overnight. Cells were then washed twice with PBS, and DAPI staining was applied to the cells. The percentage of stained and photographed cells was counted. The percentage of blue cells in a total of 800 counted cells was evaluated for each experiment.

3.2.14 In vivo experiments

Animals used for detection of x-gal positive cells in vivo were NOD.SCID CB-17 mice, between 8 and 10 weeks of age. All the mice were bred in the ITG (Institute for Toxicology and Genetics), part of the KIT (Karlsruhe Institute of Technology) animal facility under full specific pathogen free (SPF) conditions.

MCF-7 cells (5×10^6 cells/ per animal) were injected into the breast. The mice were injected intravenously with 1mg/ml estrogen every week to support tumor growth. Every two days up to 6 days tumors were subcutaneously injected with 100 μl of 2 mM hyperforin, PBS and the solvent (10% DMSO). All tumor tissues obtained from animals were embedded in OCT (Sakura Finetek) for cryosections.

3.2.15 Tissue Processing – OCT

After tissue dissection, the samples were either fixed in 4% PFA on ice for 5-10 minutes or simply washed for 5 minutes in 1x PBS, depending on the analysis to be performed. The tissues were placed in cryomolds, then overlaid with OCT, and frozen on dry ice.

3.2.16 X-gal staining in tissue

OCT-embedded tissues were cut into 5 μ M thick frozen sections, dried at RT overnight, then fixed in for 30 min at RT. The fixative consisted of 10.8 ml 37% formaldehyde, 1.6 ml 25% glutaraldehyde and PBS added up to a volume 200 ml.

The sections were subsequently washed three times with PBS for 2 min, then immersed in x-gal buffer (1mg/ml x-gal, 0.12mM $K_3Fe[CN]_6$, 0.12mM $K_4Fe[CN]_6$, 1mM $MgCl_2$ adjusted to pH 6.0 with PBS) and incubated for 24h at 37°C in a water bath. The sections were then washed with PBS and stained with 1 μ g/ μ l DAPI for 5 min at RT. The slides were washed with PBS twice, and were then analysed using the AxioVision Image 1 microscope (Zeiss).

3.2.17 Cell death detection ELISA

Endothelial and tumor cells at a confluency of ~ 50% and were treated with hyperforin or DMSO as a control for 1, 2 and 6 days. Levels of apoptosis as assessed by release of oligonucleosomes into the cytoplasm were quantified using the cell death detection ELISA kit (Roche) according to the manufacturer's instructions.

3.2.18 Quantitative assay of senescence-associated β -galactosidase activity using cell extracts by MUG (4-Methylumbelliferyl β -D-Galactopyranoside)

Cells grown in 6-well plates were washed six times with phosphate-buffered saline to remove all traces of protein from the growth medium. Cells were then lysed by the addition of 450 μ l of 1x lysis buffer (5mM 3-[(3-cholamidopropyl)dimethylammonio]-1-propanesulfonate [CHAPS], 40 mM sodium phosphate, 0.5 mM benzamidine and 0.25 mM phenylmethanesulfonyl fluoride [PMSF], pH 6.0). Cells were scraped, transferred to a 1.5 ml tube, vortexed vigorously and centrifuged for 5 min at 12000g.

The clarified supernatant was kept on ice until use. The reaction buffer at 2x strength consisted of 40 mM citric acid, 40 mM sodium phosphate, 300 mM NaCl, 10mM β -mercaptoethanol and 4mM $MgCl_2$ (pH 6.0) with 1.7mM of 4-methylumbelliferyl- β -D-galactopyranoside (MUG) added immediately prior to use from a 34mM stock in dimethyl sulfoxide.

Clarified lysate (150µl) was mixed with 150µl of 2 x reaction buffer and placed at 37°C for 30min. At the indicated times, 50µl of the reaction mix were added to 500µl of 400mM sodium carbonate stop solution, and stored at 4°C until measurement of fluorescence. The carbonate-terminated reaction mix was read at 150µl per well in a 96-well plate using a Tecan GENios automated plate reader with excitation at 360nm, and emission at 465nm.

3.2.19 Statistics

In all presented graphs error bars represent the standard error of the mean. Statistical significance was evaluated using a two-tailed student's t-test. A p-value of less than 0.05 was considered significant. In all the graphs where a statistical analysis is shown, the following symbols were used:

* = $P \leq 0.05$

** = $P \leq 0.01$

*** = $P \leq 0.001$

4 RESULTS

4.1 Senescence induction by hyperforin and aristoforin

4.1.1 Induction of senescence in endothelial cells

As previously described, the group of Prof. Sleeman has demonstrated that hyperforin and aristoforin possess anti-proliferative properties at concentrations less than 10 μM , while higher concentrations of these agents induce apoptosis in LECs (Rothley et al, 2009). To investigate the hypothesis that concentrations of less than 10 μM induce senescence, I cultivated human umbilical vein endothelial cells (HUVECs) with different concentrations of hyperforin and aristoforin, then quantified levels of senescence. As a positive control, HUVECs were treated with sirtinol, a SIRT1 inhibitor that induces senescence (Grozing et al, 2001).

HUVECs were treated with hyperforin or aristoforin at a concentration of 5, 6, 7, 8, 9 and 10 μM or with 50 μM sirtinol for 4, 6 and 9 days. Because hyperforin, aristoforin and sirtinol were dissolved in DMSO, control cells were treated with DMSO alone. The number of senescent cells was measured by x-gal staining (Demri et al, 1995). In comparison to untreated and DMSO-treated HUVECs, sirtinol strongly induced senescence in a time-dependent manner (Figure 7, A). Low concentrations of aristoforin (5 μM) induced a time-dependent increase in the number of senescent cells (Figure 1, A). However, increasing concentrations of aristoforin (6 -10 μM) progressively induced lower levels of senescence (Figure 7, A). Similar results were obtained for hyperforin-treated HUVECs, as hyperforin at 5 μM provided the highest induction of senescence in HUVECs after 9 days of treatment (Figure 7, B), while higher hyperforin concentrations (6-10 μM) induced less pronounced senescence induction (Figure 7, B).

In summary, hyperforin and aristoforin both induce senescence in HUVECs in a concentration- and time-dependent manner at concentrations that do not efficiently induce apoptosis. The reduced incidence of senescent cells with higher concentrations may be due to increasing induction of apoptosis.

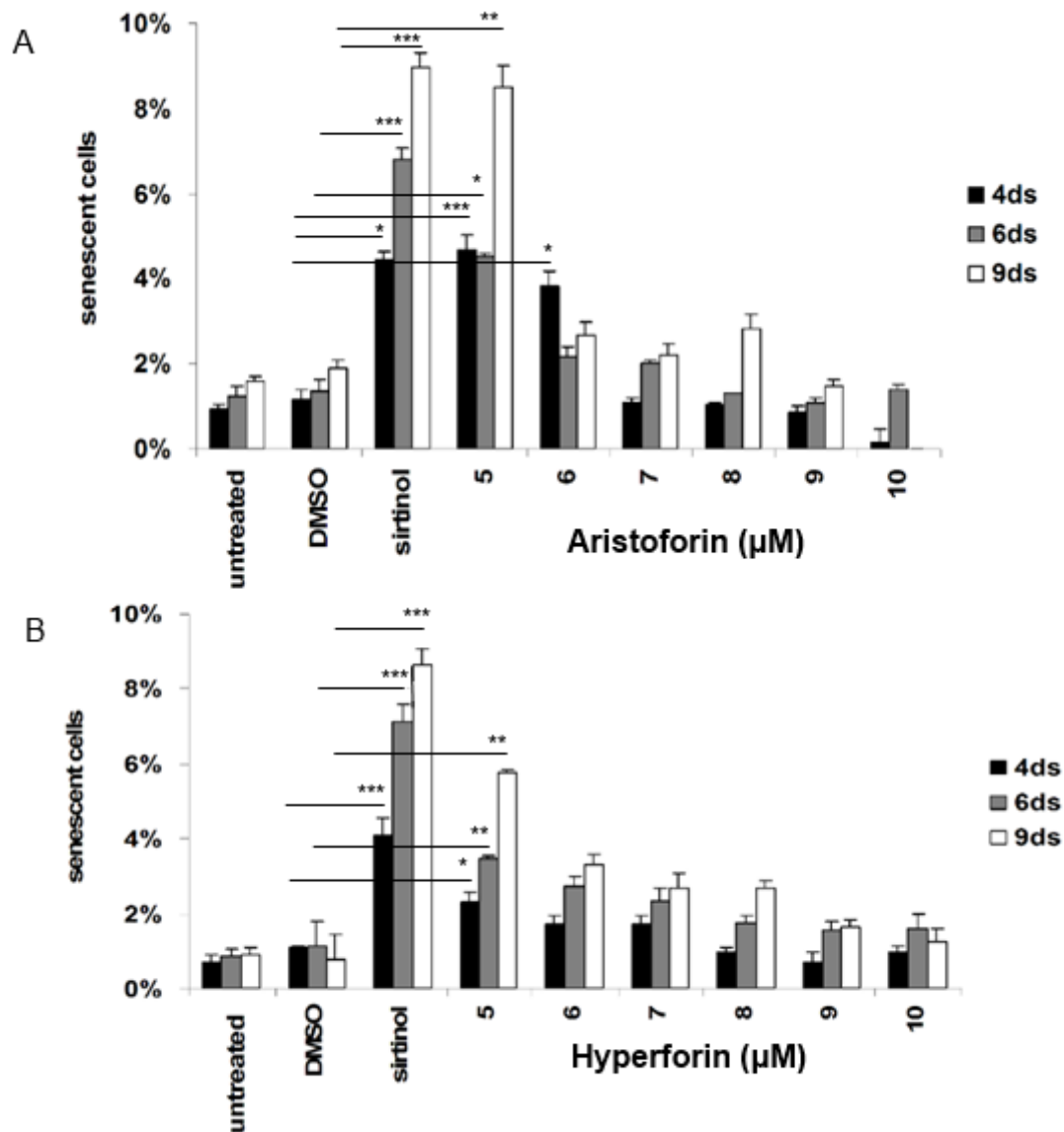


Figure 7 - Induction of senescence by hyperforin and aristoforin in HUVECs

Human umbilical vein endothelial cells were treated with different concentrations of hyperforin or aristoforin at concentrations between 3-10 μM for 4 to 9 days; the treatment was terminated using x-gal staining. A) X-gal staining in HUVECs by aristoforin shows maximal senescence induction using 5 μM aristoforin for 9 days. N=3; the error bars represent standard error. * $p \leq 0.05$. B) X-gal staining in HUVECs by hyperforin shows a significant increase in the number of senescent cells when 5 μM of hyperforin was applied for 9 days. N=3; the error bars represent standard error. * $p \leq 0.05$.

4.1.2 Antiproliferative potential of hyperforin against cancer cells is due in part to senescence induction

Hyperforin inhibits proliferation of human tumor cells with an IC_{50} of 3 to 15 μM (Schempp et al, 2002). To determine whether hyperforin also induces senescence in human tumor cells, first I tested the tumor cell line T47D (breast cancer cells) with

different low concentrations of hyperforin for certain time periods. The quantification of senescent cells was performed using x-gal staining. High levels of spontaneous senescence were observed in untreated and DMSO-treated T47D cells. Nevertheless, significantly increased numbers of senescent cells were observed after 6 days of treatment with 3 and 5 μM of hyperforin. The use of 8, 10, 12 and 15 μM hyperforin resulted in reduced senescence compared to 3 and 5 μM hyperforin (Figure 8).

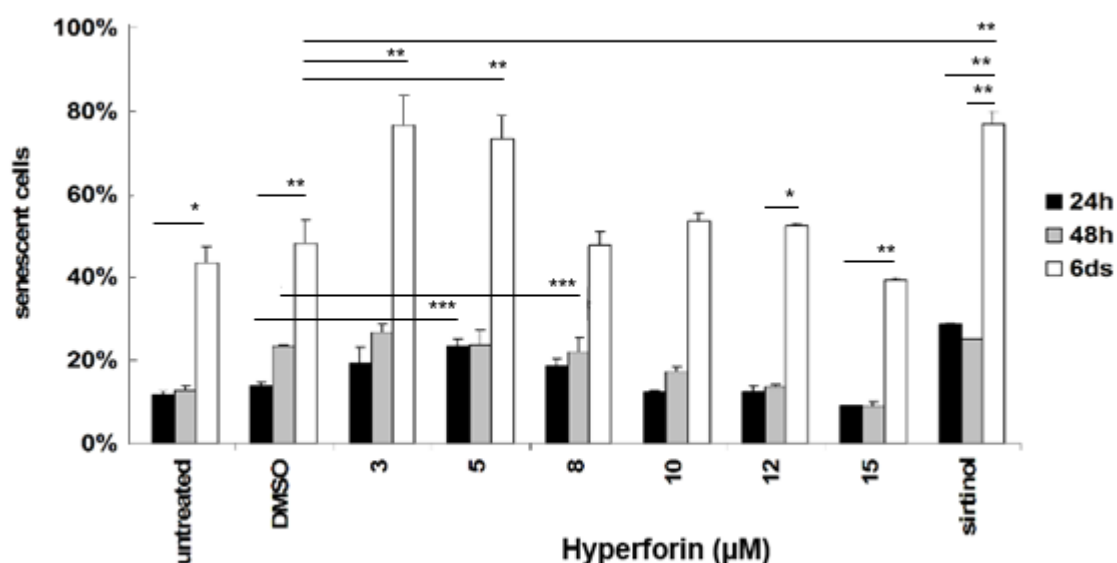


Figure 8 - Dose- and time-dependent senescence induction in the T47D cell line via hyperforin

X-gal analysis of T47D cells treated with 3-15 μM hyperforin for 24 h, 48 h and 6 days. The level of senescent cells in hyperforin-treated T47D cells, which were treated by 3 and 5 μM , is significantly induced after 6 days compared to 24 and 48 h of treatment and also compared to negative controls including untreated and DMSO-treated cells. N=3; the error bars represent standard error. * $p \leq 0.05$.

Similar to the case with HUVECs, hyperforin-induced senescence in T47D cells was progressively less pronounced at concentrations above 5 μM . As 15 μM hyperforin can induce apoptosis in tumor cell lines (Schempp et al, 2002), the reduced induction of senescence may be due to increasing levels of apoptosis induction. To determine if this is the case, T47D cells were treated with DMSO, 50 μM sirtinol or varying concentrations of hyperforin (the substances were refreshed every two days, up to 6 days), then the induction of apoptosis was assessed using a quantitative

oligonucleosome release assay (Roche). I observed no significant induction of apoptosis in untreated, DMSO-treated cells or in hyperforin-treated cells at any of the concentrations used, but a slight tendency of apoptosis induction was seen in sirtinol-treated T47D cells (Figure 9).

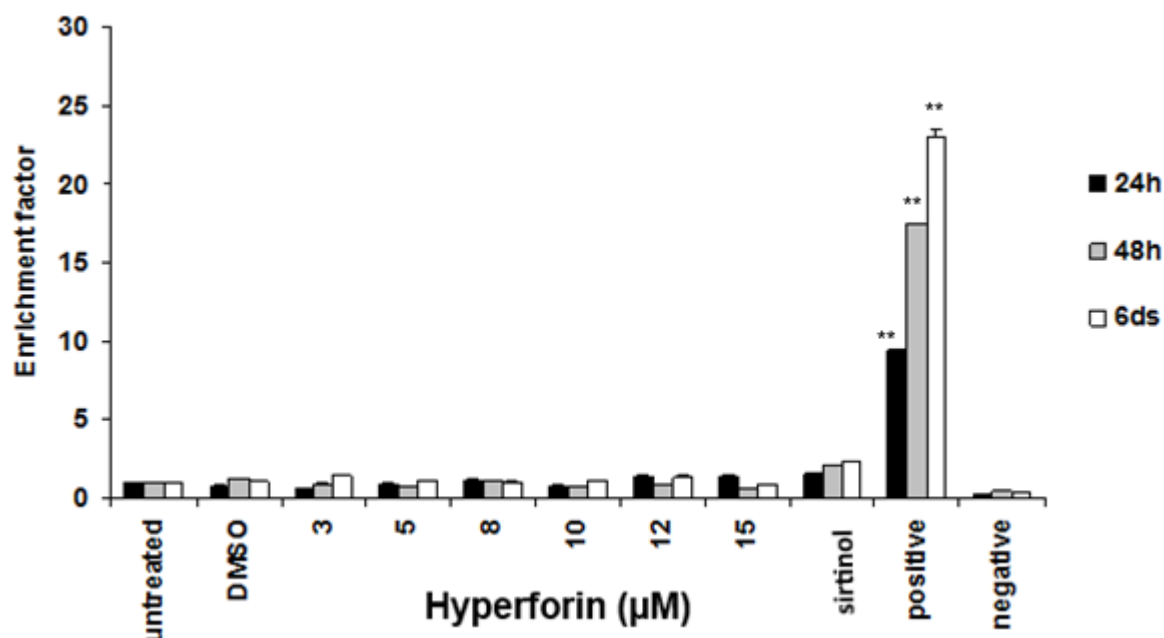


Figure 9 - Dose- and time-dependent inductions of apoptosis using hyperforin in T47D cells

Quantitative oligonucleosome release assay of T47D cells treated with hyperforin at different concentrations. There is little apoptosis in untreated T47D cells as well as in DMSO-treated and 3-15 μM hyperforin treated cells. There is a tendency of apoptosis induction at 50 μM sirtinol. The positive control from the kit shows a high level of apoptotic cells. The rate of apoptosis is reflected by the enrichment of nucleosomes in the cytoplasm shown by the value of the y-axis. N=3; the error bars represent standard error.

4.1.3 Senescence induction using hyperforin and aristoforin in different tumor cell lines

For both HUVECs and T47D cells, treatment with hyperforin concentrations of around 3 - 5 μM for 6 days were found to optimally induce senescence. Next I determined whether this is generally true for other tumor cell lines.

A panel of cancer cell lines was treated with DMSO, sirtinol (50 μM), or 5 μM hyperforin or aristoforin for 6 days, with a medium change every 48h as before. Under these conditions, hyperforin induced senescence significantly in ACC57

cervical carcinoma cells, HCT116 and SW480 colorectal cancer cells, and MCF-7 breast cancer cells, but not in PC3human prostate cancer cells (Figure 10). As MCF-7 cells showed the most pronounced hyperforin-induced senescence, these cells were chosen for subsequent in vivo and mechanistic studies.

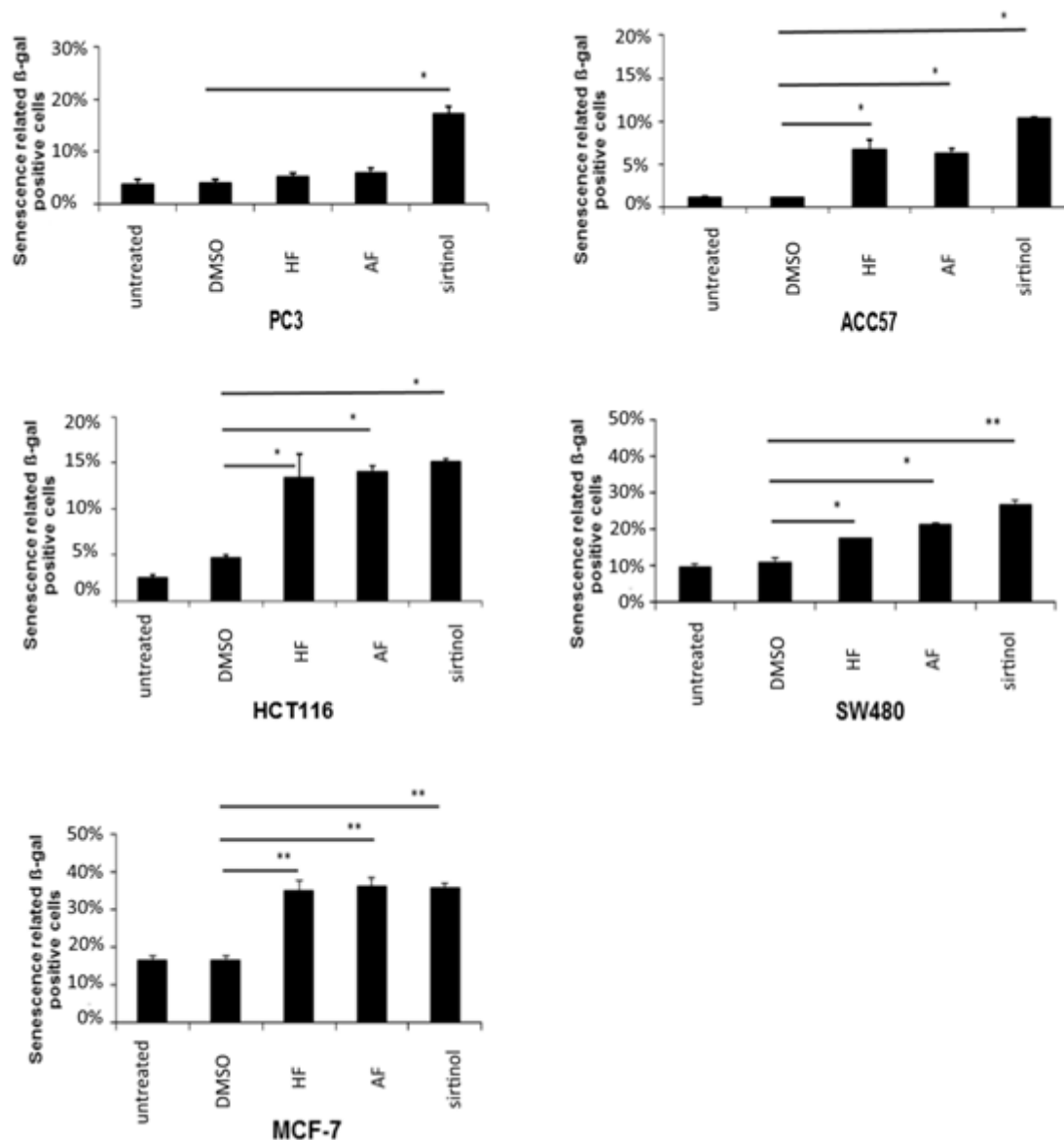


Figure 10 -Senescence induction by hyperforin and aristoforin in different cancer cells

The indicated tumor cell lines were treated with DMSO, sirtinol (50 μ M), or 5 μ M hyperforin or aristoforin for 6 days, with a medium change every 48 h. After subsequent x-gal staining, the percentage of x-gal-positive cells was evaluated. The mean and standard error of 4 independent samples is presented. *p ≤ 0.05.

4.1.4 Hyperforin induces senescence in vivo

To determine whether hyperforin can induce senescence in vivo, MCF-7 tumor-bearing animals were treated with hyperforin, then the presence of senescent cells in the tumor was evaluated by x-gal staining of frozen tumor sections. To this end, mice were injected subcutaneously with MCF-7 cells. Tumors were allowed to develop for 4 weeks, then the animals were treated intraperitoneally with PBS, DMSO or 2 mM hyperforin every day for 6 days. Tumors were then excised and prepared for cryo sectioning. X-gal staining was performed on 5 μ M sections for senescent cell analysis. Each section was stained with DAPI as well as x-gal. After the staining, the sections were observed under the microscope and both DAPI and x-gal positive cells were counted separately to assess the percentage of x-gal positive (senescent) cells compared to the total number of DAPI-stained cells. Compared to controls, hyperforin treatment resulted in a significant increase in the presence of senescent cells (Figure 11), with control tumors containing around 0.7% senescent cells compared to more than 4% in hyperforin-treated tumors.

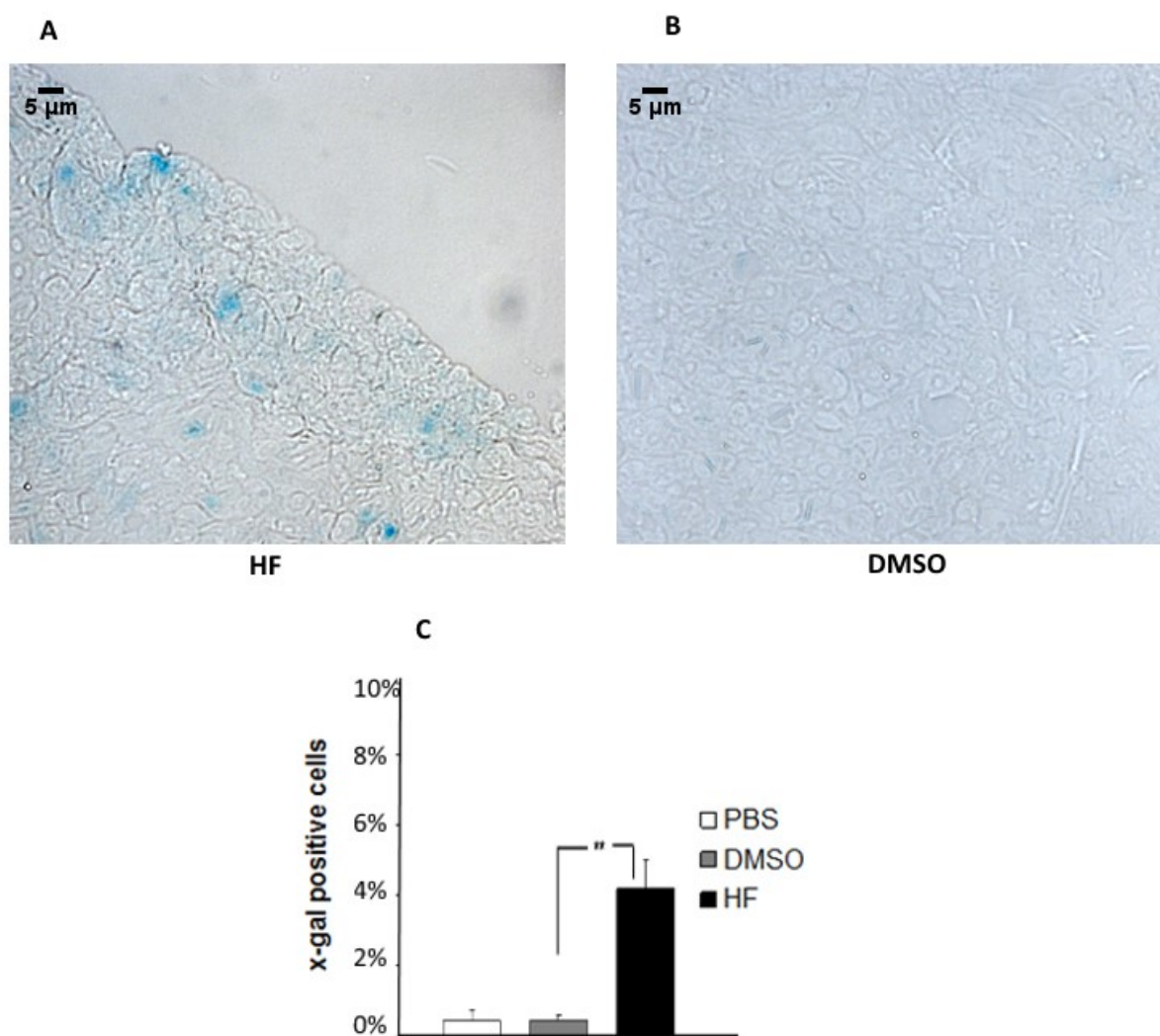


Figure 11 - Detection of x-gal positive cells in tumor tissue using hyperforin

A) X-gal staining shows the positive x-gal stained cells in hyperforin-treated tumor tissue from mice. B) X-gal staining in DMSO treated tumor tissue from mice. C) X-gal staining shows the level of x-gal positive cells in mouse tumor tissue, which had been treated with PBS, DMSO or hyperforin for 6 days. The level of x-gal positive cells in the tissue treated with hyperforin is significantly increased in comparison to the DMSO control. $N=5$; the error bars represent standard error. $*p \leq 0.05$.

4.2 Molecular mechanism of hyperforin-induced senescence

Next I set out to determine the molecular mechanism by which HF and AF induces senescence. As outlined in detail in the Introduction, a number of candidate factors through which hyperforin could induce senescence can be identified from the literature. Hyperforin inhibits SIRT1 activity (Gey et al, 2007), and induces Noxa

expression, a direct target of the p53 gene that regulates senescence induction. Experiments were therefore performed to determine whether these factors play a role in senescence induction by hyperforin treatment.

4.2.1 Role of SIRT1

RSV activates SIRT1 activity (Howitz et al, 2003). I therefore reasoned that if hyperforin/aristofofin induces senescence by inhibiting SIRT1, then RSV should counteract hyperforin-induced senescence. To determine if this is the case, HUVECs, LECs and different tumor cells were treated in the presence or absence of RSV with a senescence-inducing concentration of hyperforin or aristofofin (5 μ M), or with sirtinol. As before, cells were treated for up to 6 days, and the medium was changed every 48h. The cells were then stained by x-gal to detect senescent cells.

Untreated and DMSO-treated HUVECs and LECs exhibited similar levels of senescent cells as untreated cells, as didresveratrol-only treated HUVECs and LECs (Figure 12). In contrast, senescence was strongly induced by hyperforin, aristofofin and sirtinol treatment of HUVECs and LECs as expected (Figure 12). Importantly, RSV treatment significantly reduced senescence induced by hyperforin, aristofofin and sirtinol (Figure 12). These data provide evidence that hyperforin and aristofofin induce senescence by inhibiting the activity of SIRT1.

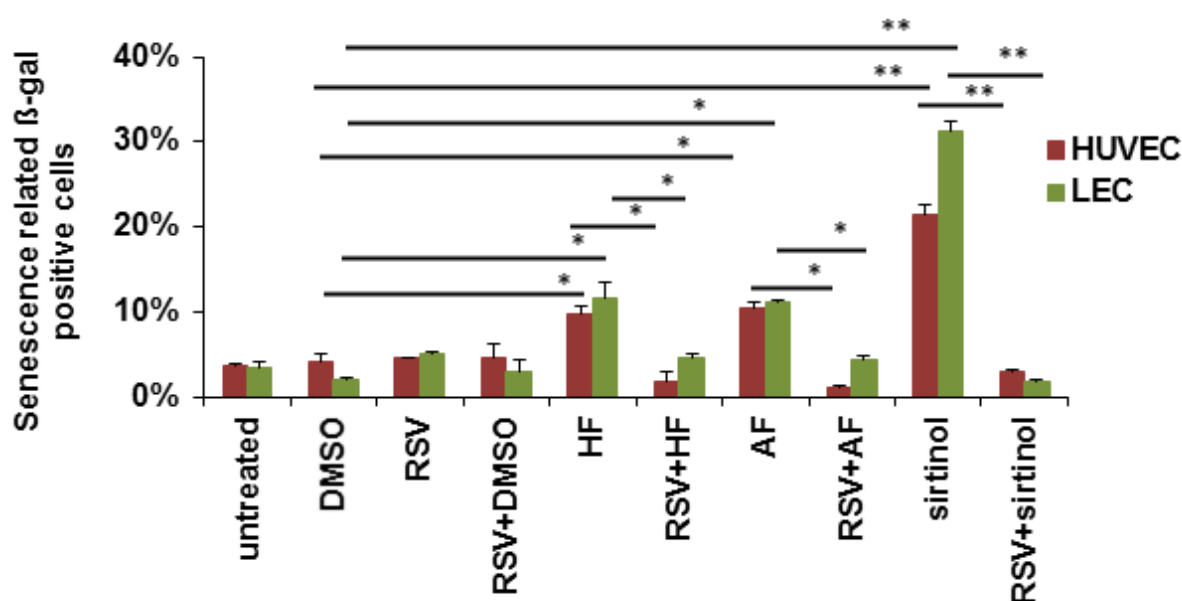


Figure 12 - Hyperforin- and aristofofin-induced senescence is suppressed by the sirtuin activator RSV in ECs

HUVECs and LECs were treated in the presence or absence of RSV with hyperforin or aristoforin (5 μ M), or with sirtinol for 6 days, and the medium was changed every 48 h. The cells were then stained by x-gal to detect senescent cells, and the percentage of x-gal-positive cells was evaluated. The mean and standard error of 3 independent samples is presented. * $p \leq 0.05$.

Similar experiments were performed with different cancer cell lines (Figure 13). For some of these lines, notably MCF-7 and T47D, RSV was able to suppress hyperforin and aristoforin-induced senescence (Figure 13). However, for other cell lines such as ACC57 and SW480, while hyperforin and aristoforin significantly induced senescence, RSV was unable to reverse this effect (Figure 13). Together these data suggests that hyperforin and aristoforin may induce senescence at least partially by inhibiting SIRT1 in ECs and some tumor cells, but that hyperforin and aristoforin can also induce senescence via other mechanisms. In view of the observations I therefore first investigated the possible role of SIRT1 in hyperforin/aristoforin-induced senescence before expanding the analysis to explore other possible mechanisms.

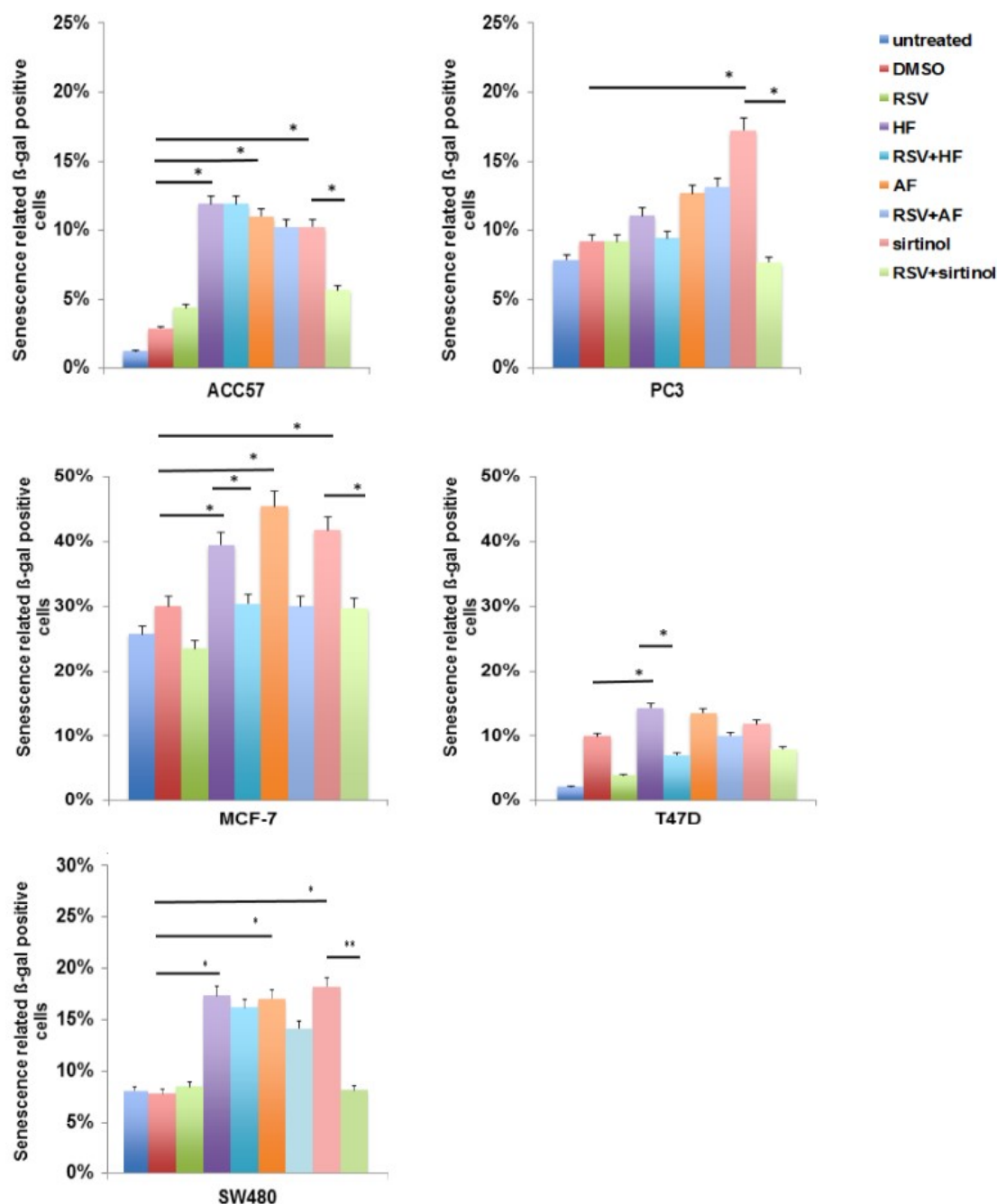


Figure 13 -Hyperforin- and aristoforin-induced senescence can be inhibited by the sirtuin activator RSV in some cancer cells

The indicated tumor cells were treated in the presence or absence of RSV with hyperforin or aristoforin (5 μ M), or with sirtinol for 6 days, and the medium was changed every 48 h. The cells were then stained by x-gal to detect senescent cells, and the percentage of x-gal-positive cells was evaluated. The mean and standard error of 3 independent samples is presented. * $p \leq 0.05$.

4.2.1.1 Effect of SIRT1 inactivation on senescence induction

If inhibition of SIRT1 is responsible for hyperforin-mediated senescence, I reasoned that SIRT1 knockdown should also induce senescence, and hyperforin should not

further increase senescence over and above that induced by hyperforin. To determine if this is the case, I knocked down SIRT1 expression in MCF-7 cells using a retroviral shRNA construct. Then the level of senescent cells induced by hyperforin in the absence of SIRT1 was analyzed in comparison with the senescence level in HF-treated parental cells.

As demonstrated in Figure 14, SIRT1 protein could not be detected using western blotting in MCF-7 cells transfected with shRNA against SIRT1, whereas a robust signal was found in both MCF-7 parental cells and MCF-7 transfected with scrambled RNA, demonstrating the efficiency of the knockdown. Treatment of cells with hyperforin and aristoforin also reduced SIRT1 expression compared to DMSO-treated control cells (Figure 14).

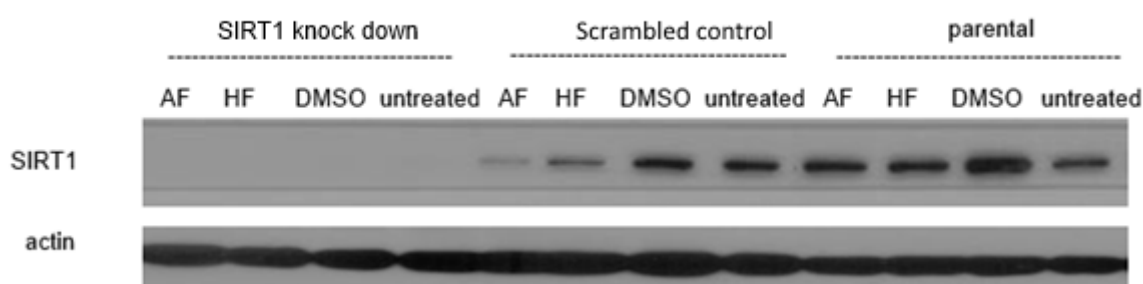


Figure 14 - Western blotting of MCF-7 cells related to the SIRT1 expression by hyperforin treatment

Western blot analysis of parental, scrambled control and knock down of SIRT1 in MCF-7 cells using polyclonal rabbit-anti-SIRT1 antibody. Actin is used as a loading control.

MCF-7 cells with knockdown of SIRT1 showed a significant increase in spontaneous senescence (Figure 15). However, hyperforin and aristoforin strongly increased senescence over and above these levels. These data suggest that the inhibitory effect of hyperforin and aristoforin on SIRT1 is not sufficient to explain senescence induction by these compounds, and additional molecular mechanisms must exist.

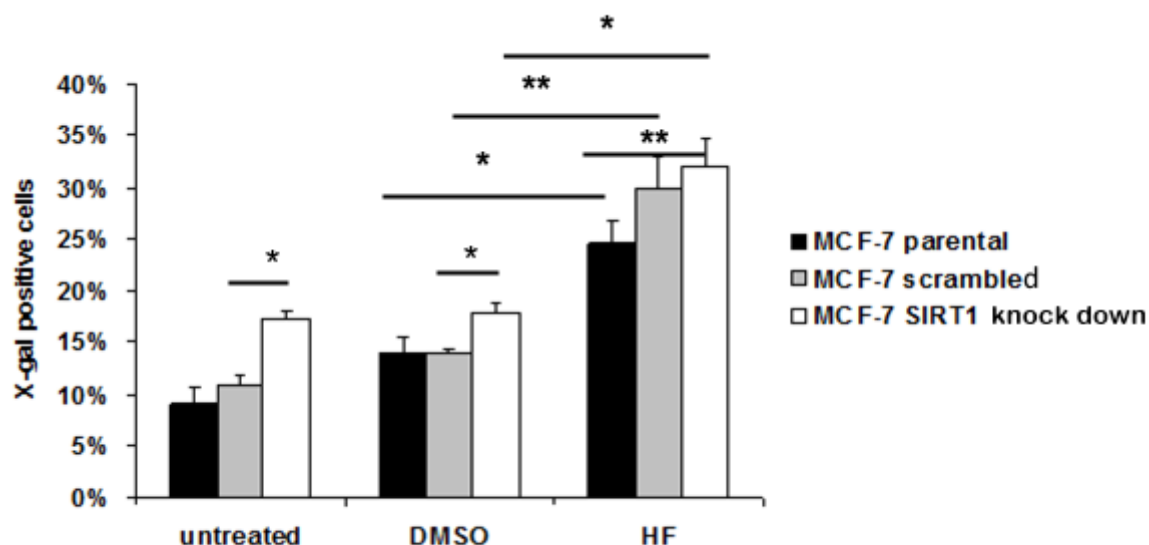


Figure 15 - Knockdown of SIRT1 expression in MCF-7 cells does not inhibit hyperforin-induced senescence

X-gal analysis of parental, scrambled control and knock down of SIRT1 in MCF-7 cells treated by DMSO and hyperforin. N=4; the error bars represent standard error. *p ≤ 0.05.

4.2.2 Hyperforin induces Noxa expression at senescence-inducing concentrations

Hyperforin induces Noxa expression in chronic lymphatic leukemia cells and induces apoptosis (Zaher et al, 2002). However, to date Noxa expression has not been associated with senescence. Nevertheless, it is a direct p53 target, and p53 regulates senescence. Therefore I reasoned that Noxa expression may play a role in hyperforin-induced senescence. To determine whether this is the case, I first examined whether hyperforin is able to induce Noxa expression at senescence-inducing concentrations (Figure 16). As a positive control, the cells were also treated with 18 μM of hyperforin for 24h which is sufficient to induce Noxa expression (Zaher et al, 2002). As another control, cells were transfected with a Noxa expression plasmid.

Induction of Noxa expression by 8 μM hyperforin was evident on the western blot 24 h, 4 and 6 days after treatment (Figure 16), showing that Noxa is also expressed in response to hyperforin at senescence-inducing concentrations.

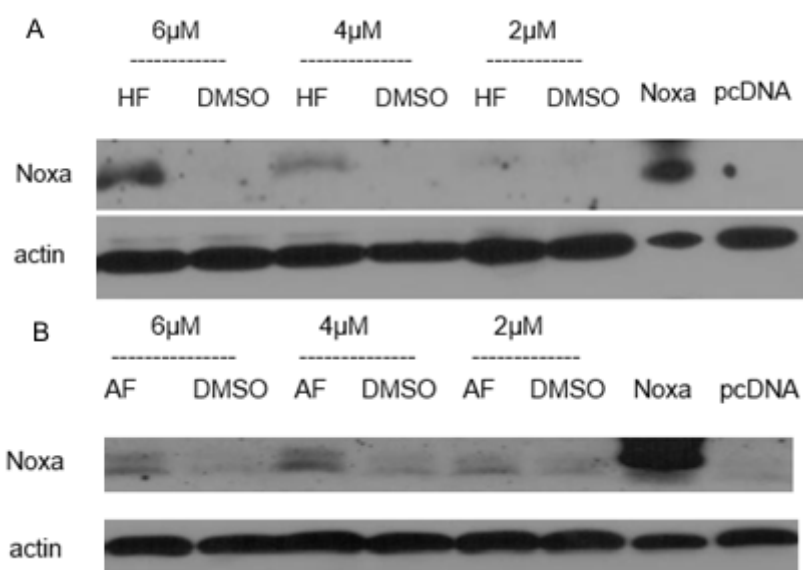


Figure 17 - Western blot analysis of Noxa induction by hyperforin and aristoforin at low concentrations

A) Western blot analysis of hyperforin treated MCF-7 cells using monoclonal mouse-anti-Noxa antibody. B) Western blot analysis of aristoforin treated MCF-7 cells using monoclonal mouse-anti-Noxa antibody. Actin was used as a loading control. Positive control shows MCF-7 cells transfected with pcDNA-Noxa.

4.2.2.1 Knock down of Noxa expression by short hairpin ribonucleic acid (shRNA) suppresses hyperforin-induced senescence

To investigate whether Noxa plays a functional role in the induction of senescence by hyperforin, I used a loss of function approach. Specifically, Noxa expression was knocked down in MCF-7 cells using a shRNA against Noxa, and then the effect of the knockdown on hyperforin-induced senescence was evaluated.

First, MCF-7 cells were transfected with five different Noxa shRNAs. Knock down efficiency of Noxa was checked by Western blot. Only Noxa shRNA 2 was found to suppress Noxa expression (Figure 18).

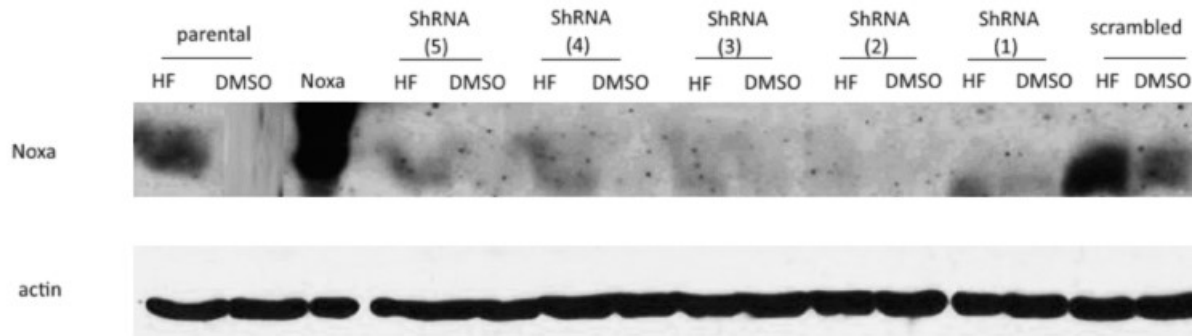


Figure 18 - Western blot analysis of Noxa induction using shRNA against Noxa by hyperforin treatment

Western blot analysis of Noxa knock down efficiency by hyperforin treatment in MCF-7 cells using a monoclonal mouse-anti-Noxa antibody (upper panel). Noxa shRNA no. 2 shows a clear knockdown of Noxa. Actin was used as a loading control (lower panel).

Knockdown of Noxa expression compared to parental cells and scramble control cells is shown in Figure 19. Hyperforin treatment increased Noxa expression in the parental and scramble control cells, but not in the Noxa knockdown cells (Figure 18).

Loss of Noxa sufficed to significantly reduce the background levels of senescence. Importantly, loss of Noxa also strongly inhibited hyperforin-induced senescence (Figure 19). These data suggest that Noxa is a key regulator of hyperforin-induced senescence.

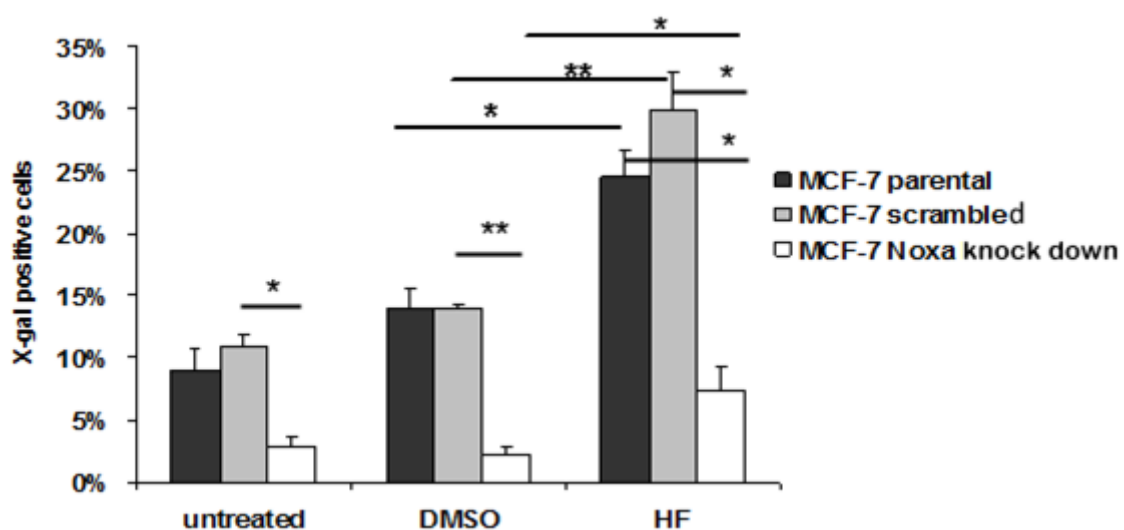


Figure 19 - Functional analysis of Noxa expression

X-gal analysis of parental, scrambled control and knock down of Noxa in MCF-7 cells treated by DMSO and hyperforin. N=4; the error bars represent standard error. * $p \leq 0.05$.

4.2.2.2 Noxa induction by hyperforin is not dependent on p53

Noxa is a target gene of p53. Furthermore, p53 has been suggested to play a central role in SIRT1-mediated cell senescence (Yiand Luo, 2010). Therefore I next investigated whether p53 is required for hyperforin-mediated Noxa upregulation.

To answer this question I used two related human colon carcinoma cell lines, namely HCT+/+ with wild type p53, and a derivative cell line with a p53 deletion in both alleles (HCT-/-). The cell lines were treated with hyperforin or aristoforin, then senescence induction and Noxa and p53 expression were evaluated.

Hyperforin and aristoforin both significantly induced senescence in HCT+/+ cells, whereas no induction was observed in HCT-/- cells (Figure 20, A). Western blot analysis confirmed that no p53 protein is present in HCT-/- cells, while HCT+/+ showed a strong expression of p53. HCT116 cells served as a positive control (Figure 20, B). Furthermore, there was no significant effect on p53 protein levels after incubation of the cells with 6 μ M hyperforin for 48 h. However, hyperforin-treated HCT116, HCT+/+ and HCT-/- cells all showed strong Noxa expression (Figure 20, B).

Together, these data suggest that p53 is required for hyperforin- and aristoforin-induced senescence, but not for induction of Noxa expression in response to these compounds. Moreover, these data indicate that while Noxa is required for hyperforin-induced senescence (see Figure 20), in the absence of p53 its expression is not sufficient to mediate senescence by hyperforin.

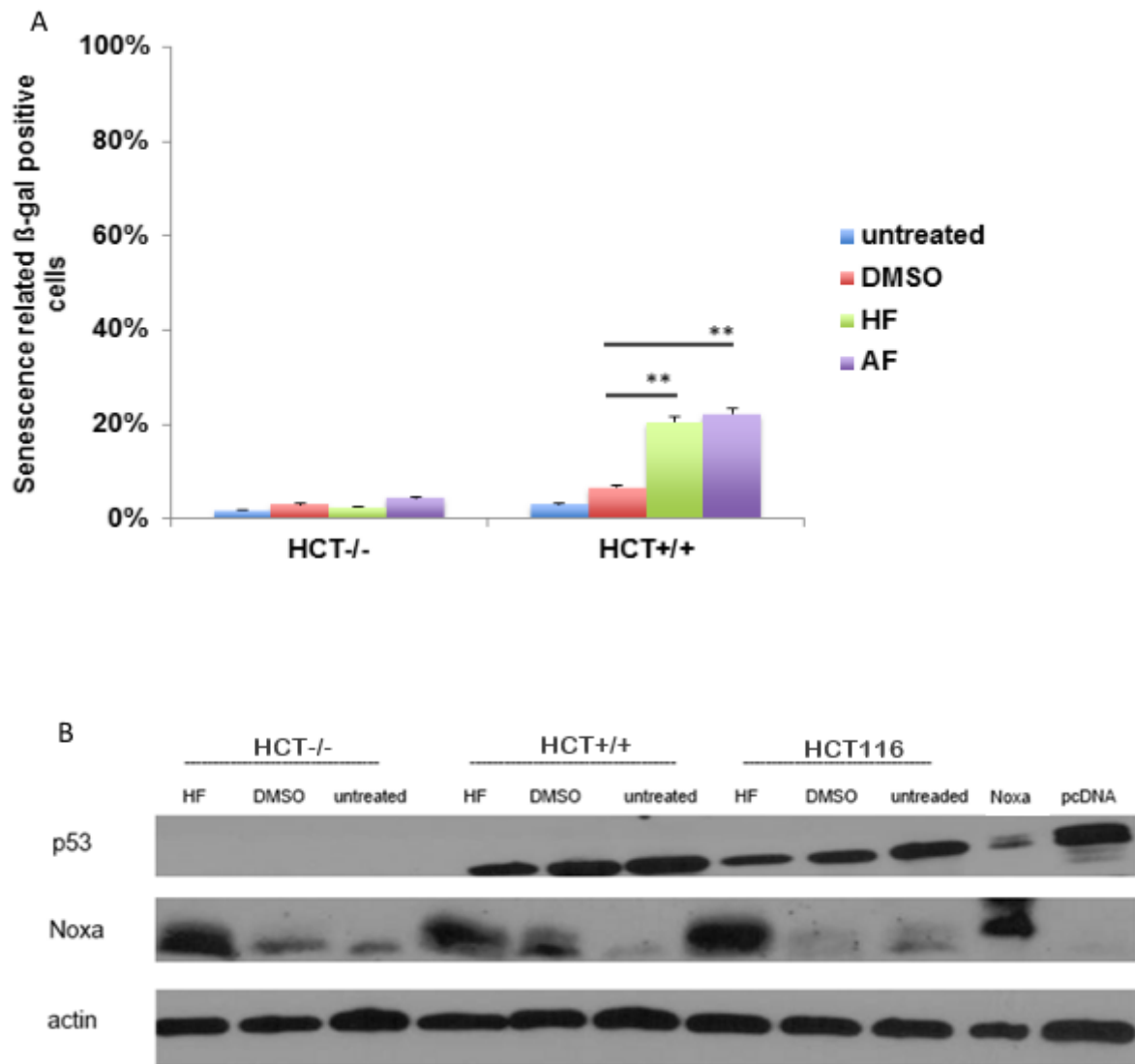


Figure 20 - Hyperforin and aristoforin induce senescence in a p53-dependent manner

A) X-gal analysis of the indicated cell lines after hyperforin and aristoforin treatment (6 μ M) for 48 h. N=4; the error bars represent standard error. * $p \leq 0.05$. B) Western blot analysis using monoclonal mouse-anti-p53 and monoclonal mouse-anti-Noxa antibodies to detect p53 and Noxa expression in the indicated cell lines. Actin is used as a loading control.

I also investigated whether RSV is able to suppress hyperforin- and aristoforin-induced senescence in HCT+/+ cells, which proved to be the case (Figure 21). These data therefore suggest that inhibition of sirtuin activity also contributes to hyperforin- and aristoforin-induced senescence in these cells.

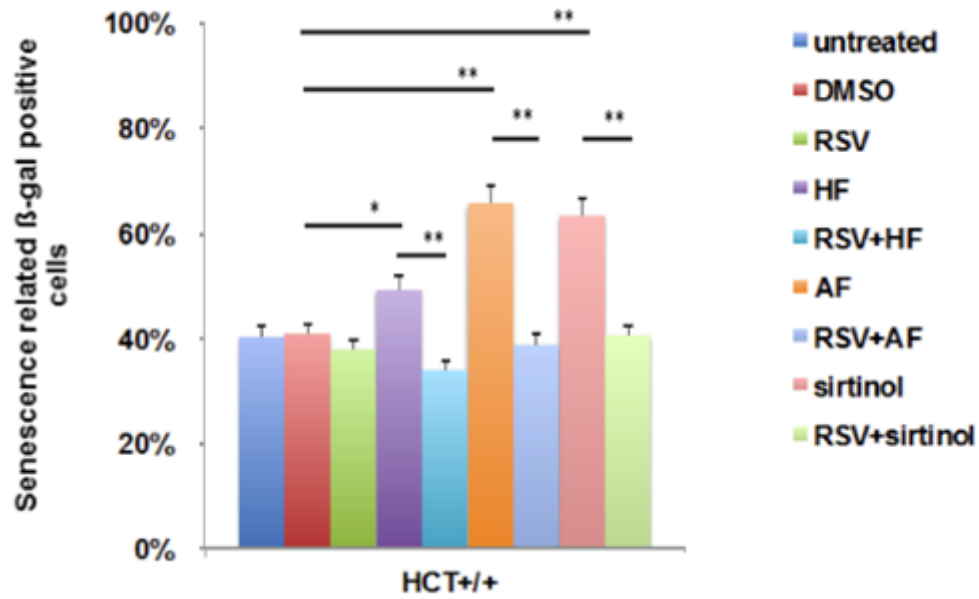


Figure 21 - Hyperforin- and aristoforin-induced senescence in HCT+/+ cells can be inhibited by the sirtuin activator RSV

HCT+/+ cells were treated in the presence or absence of RSV with hyperforin or aristoforin (5 μ M), or with sirtinol for 6 days, and the medium was changed every 48 h. The cells were then stained by x-gal to detect senescent cells, and the percentage of x-gal-positive cells was evaluated. The mean and standard error of 3 independent samples is presented. * $p \leq 0.05$.

4.3 Development of improved methods to analyze senescent cells

Quantification of x-gal staining to analyze senescent cells using microscopy is time-consuming and subjective, as the cells need to be evaluated by eye and counted. I therefore set out to develop a flow cytometry-based technique to quantify SA- β gal activity. For this purpose I used 5-dodecanoyl-aminofluorescein di- β -D-galactopyranoside (C_{12} FDG), a membrane permeable, non-fluorescent substrate of β -galactosidase, which upon hydrolysis by SA- β gal becomes fluorescent and membrane impermeable (Kurz et al, 2000). Cell senescence was assessed in parallel by measuring both SA- β gal activity with cytochemistry (x-gal staining) and flow cytometry (C_{12} FDG staining) to cross-validate the technique.

4.3.1 Rapid flow cytometric method for measuring senescence associated beta-galactosidase activity using C_{12} -FDG

HUVEC cells were treated with 50 μ M sirtinol for 24 h to induce senescence, then subdivided into two groups. One group was analysed without further treatment. The other group was treated for 1 h with the pH modulator bafilomycin A1 to optimize β -galactosidase activity. The cells were then either incubated with C_{12} FDG for 10 min and prepared for FACS analysis, or stained with x-gal.

As seen in Table 1, as expected the number of x-gal positive cells without pH optimization is lower compared to that in the pH-optimized cells. Levels of x-gal positive HUVEC cells were comparable to those obtained in previous experiments. In contrast, a very high level of C_{12} FDG-positive cells was obtained regardless of pH optimization (Table 1). Crucially, the background signal in untreated cells is very high, which is not the case in x-gal staining. These data show that C_{12} FDG staining is not specific and unsuitable for the quantification of senescent cells using FACS. Therefore, other approaches were taken to quantify senescent cells using the fluorescence markers LysoTracker yellow.

	C₁₂FDG-positive (%)	X-gal staining-positive (%)
	with/without bafilomycin	with/without bafilomycin
untreated	79.6/ 50.8	7.8/ 1
DMSO	81.4/ 50.2	8.2/ 1.7
sirtinol	87.8/ 76.3	26.6/ 11.1

Table 1 - Quantification of senescent cells using x-gal staining, and parallel quantification of C₁₂FDG-stained cells using FACS analysis

The numbers indicate the percentage of positive cells in each case with and without pH optimization using bafilomycin in untreated, DMSO and sirtinol-treated HUVECs.

4.3.2 Quantification of FACS analysis of lysotracker yellow stained cells

One of the most characteristic changes in aged cells is an increase in the number and the size of lysosomes. This process is very intensive and often a large part of the cytoplasm is occupied by lysosomes. The increase in lysosomal mass is therefore a hallmark of aged cells (Keller et al, 2004; Samorajski et al, 1968). The fluorescent dye lysotracker yellow is taken up by cells and labels lysosomes, allowing the increased lysosomal mass to be quantified and used as a measure of senescence induction (Kurz et al, 2000). I therefore set out to establish a FACS-based analysis using lysotracker yellow to quantify senescent cells. To this end, HUVEC cells were treated with DMSO and sirtinol as before to induce senescence. After treatment, a portion of the cells was stained with lysotracker yellow and another portion was prepared for x-gal staining. Lysotracker yellow positive cells were quantified using FACS and the x-gal positive cells were counted under the microscope.

X-gal staining showed an induction of senescence in sirtinol treated cells as expected (Table 2). However, in FACS analysis of lysotracker yellow treated cells there was no correlation between the percentage of positive cells and treatment with sirtinol (Table 2). Thus, lysotracker yellow staining is also not a robust means of detecting senescence using FACS analysis.

	FACS analysis %	X-gal staining%
	unstained/ stained	
untreated	0.6/ 32.4	2.4
DMSO	0.1/ 5.1	4.6
sirtinol	0.3/ 15.7	8.4

Table 2 - Quantification of FACS analysis using lysotracker yellow and x-gal staining

The HUVECs were treated with DMSO and sirtinol 50 μ M for 24 h and finally stained with the dye and subjected to flow cytometry analysis. B) X-gal analysis of untreated and treated HUVECs.

4.3.3 Quantitative assay of senescence-associated β -galactosidase activity using cell extracts

I next aimed to use the ability of β -galactosidase to convert 4-methylumbelliferyl (MUG) into the fluorescent product 4-methylumbelliferone (4-MUG) as a measure of senescence using cell lysates, which can be detected using a plate reader (Gary et al, 2005). A major advantage of the MUG fluorogenic assay is that SA- β -gal is normalized on the basis of total protein, which avoids problems associated with concomitant induction of cell growth arrest or cell death, leading to changes in the number of cells present at the time of analysis. The second advantage is that the assay is much quicker compared to the x-gal assay.

To establish the assay, MCF-7 cells were treated with either DMSO or sirtinol (50 μ M) to induce senescence, then lysed after 24 h. Cell lysates were pipetted into a 96-well plate and MUG was added to the lysate. Subsequently, the levels of the fluorescent hydrolysis product 4-MUG were measured using a Tecan GENios automated plate reader. The x-gal assay was simultaneously performed with parallel samples to cross-validate the percentage of x-gal positive cells obtained in both methods.

As shown in Figure 22, A sirtinol-treated MCF-7 cells showed significantly higher levels of 4-MUG compared to DMSO treated cells. Importantly, the x-gal assay showed equivalent relative levels of senescent cells compared to the 4-MUG fluorescence assay (Figure 22, B). These data indicate that the MUG fluorogenic assay can be used

as a time-saving, sensitive and objective alternative method to x-gal staining and manual quantification.

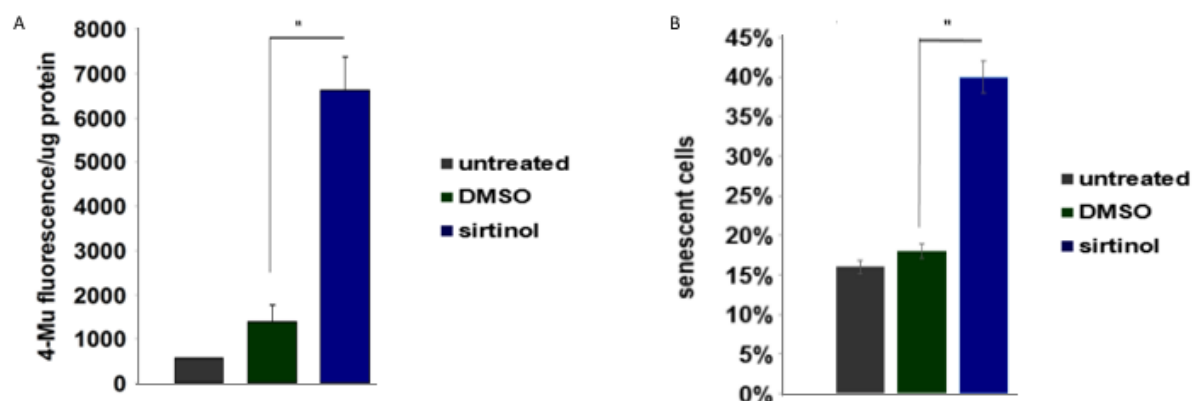


Figure 22 - Quantitative SA-β gal assay using MUG

A) MUG fluorogenic assay analysis after 24 h treatment of MCF-7 cells with 50 μM sirtinol shows a significant increase in 4-MUG fluorescence. The fluorescence intensity per μg protein in the lysate was calculated. B) Quantification of x-gal using SA-β gal assay and microscopy. N=3; the error bars represent standard error. *p ≤ 0.05.

5 DISCUSSION

In this thesis I have investigated how hyperforin and aristoforin induce cell cycle arrest in endothelial cells and tumor cells at concentrations below those required to induce apoptosis. I found that concentrations of hyperforin and aristoforin known from previous work to induce cell cycle arrest (Schempp et al, 2002; Rothley et al, 2009) were able to induce senescence in endothelial cells and tumor cells both *in vitro* and *in vivo* as measured by SA- β -gal staining. Mechanistically I obtained evidence that inhibition of SIRT1 and induction of Noxa expression by hyperforin and aristoforin play a role in the induction of senescence, and that the presence of p53 is required for hyperforin and aristoforin-induced senescence. Together these data provide further support for the notion that hyperforin and aristoforin have potential application in cancer therapy through their ability to suppress tumor growth at multiple levels.

To analyze senescent cells, the traditional x-gal staining method (Dimri et al, 1995) was used for most of this work. However, to analyse senescent cells rapidly and more specifically, I investigated the efficacy of other assays. The use of C₁₂FDG and lysotracker yellow proved to be unsuitable for quantification of senescent cells using FACS analysis. However, I found that 4-methylumbelliferyl- β -D-galactopyranoside (MUG) can be used in a rapid quantitative assay for the detection of senescent cells that is comparable with results analysed by x-gal staining.

5.1 Hyperforin induces senescence in ECs, tumor cell lines and tumors *in vivo*:

For both HUVECs, LECs and several tumor cell lines, aristoforin and/or hyperforin concentrations of 5 μ M were found to induce senescence. In all cases the most pronounced induction of senescence occurred after several days of treatment (at least 4 days, see (Figure 7, Figure 10). This presumably reflects at least in part the fact that cells enter senescence after a mitosis skip (Johmura et al, 2014), and thus in non-synchronized cell populations senescent cells accrue with a kinetic that is determined by the length of the cell cycle. Although not determined for all cell types tested, optimal senescence-inducing concentrations of hyperforin and aristoforin were 3-5 μ M (Figure 7).

Interestingly, different tumor cell lines had very different baseline levels of senescence ranging from 10% in HCT-/- and 12% in PC3 cells to 28% in MCF7 cells. Spontaneous senescence is widely observed in cancer cells, and probably reflects stochastic changes in telomere length, or microenvironmental changes (Shay and Roninson, 2004). It is notable that tumor cells with no functional p53 (PC3, Nagafuchi et al, 1989 and HCT-/-, Bunz et al, 1999) or inactivated p53 (ACC57, Akiyama et al, 1985) showed the lowest spontaneous senescence levels. This is consistent with the known role of p53 in the induction of senescence. However, hyperforin did cause visible but small increases in senescence in these p53-deficient cell lines, indicating that hyperforin probably also activates p53-independent mechanisms of senescence induction at a lower level.

It has previously been shown that hyperforin and aristoforin are able to induce apoptosis in both endothelial cells and tumor cells. Hyperforin (IC₅₀ 3-15 μ M) inhibits the proliferation of a panel of tumor cells and at 15 μ M induces apoptosis (Schempp et al, 2002). Similarly, hyperforin and aristoforin induce apoptosis of LECs at concentrations above 10 μ M (Rothley et al, 2009). Surprisingly, I was unable to detect induction of apoptosis in T47D cells even at 15 μ M, the highest concentration used (Figure 9). This may suggest that T47D cells are intrinsically resistant to hyperforin-induced apoptosis. Alternatively, the specific activities of the hyperforin preparations used may have been lower than those used in previous studies, and thus higher hyperforin concentrations may have induced apoptosis. Further work will be necessary to investigate these possibilities.

I observed the maximum induction of senescence at hyperforin and aristoforin concentrations of around 5 μ M. At higher concentrations the proportion of senescent cells decreased. Given the documented ability of both hyperforin and aristoforin to induce apoptosis at concentrations above 5 μ M (see above), the progressive reduction in the proportion of senescent cells observed at hyperforin and aristoforin concentrations above 5 μ M presumably reflect an overlap between induction of senescence and induction of apoptosis. In this scenario, apoptosis would be expected to progressively increase as hyperforin and aristoforin concentrations increase above 5 μ M, thus reducing the proportion of senescent cells. Such a mechanism could be provided by p53, as using a p53-inducible system, it has been shown that changes in p53 levels correlate with transcriptional activation of genes

involved in senescence and apoptosis. However, apoptosis was only induced above a particular p53 threshold (Kracikova et al, 2013). Further investigations will be needed to determine whether such a mechanism holds true for hyperforin-induced senescence and apoptosis.

In addition to inducing senescence in cultured cells, hyperforin also induced senescence in tumor tissue in vivo (Figure 11). These data validate the relevance of senescence induction by hyperforin in vivo in the tumor context. Importantly, they also provide support for the notion that hyperforin may have therapeutic anti-cancer applications. Previously hyperforin and aristoforin have been shown to suppress tumor growth in vivo (Rothley et al, 2009). My findings add further mechanistic insight into the action of hyperforin in the inhibition of tumor growth. Specifically, in addition to its known ability to induce apoptosis, it can also induce senescence. Currently it is not clear whether hyperforin induced senescence in vivo in tumor cells, stromal cells such as endothelial cells or both. Attempts to co-stain with x-gal and antibody markers to allow x-gal-positive cells to be characterized have so far been unsuccessful. Development of methods to allow such co-staining will be the focus of future experiments.

5.2 Molecular mechanism of hyperforin/aristoforin-induced senescence

The experiments in this thesis allow me to propose a molecular mechanism through which hyperforin and aristoforin induce senescence (Figure 23). This mechanism involves suppression of SIRT1, induction of Noxa and requires p53.

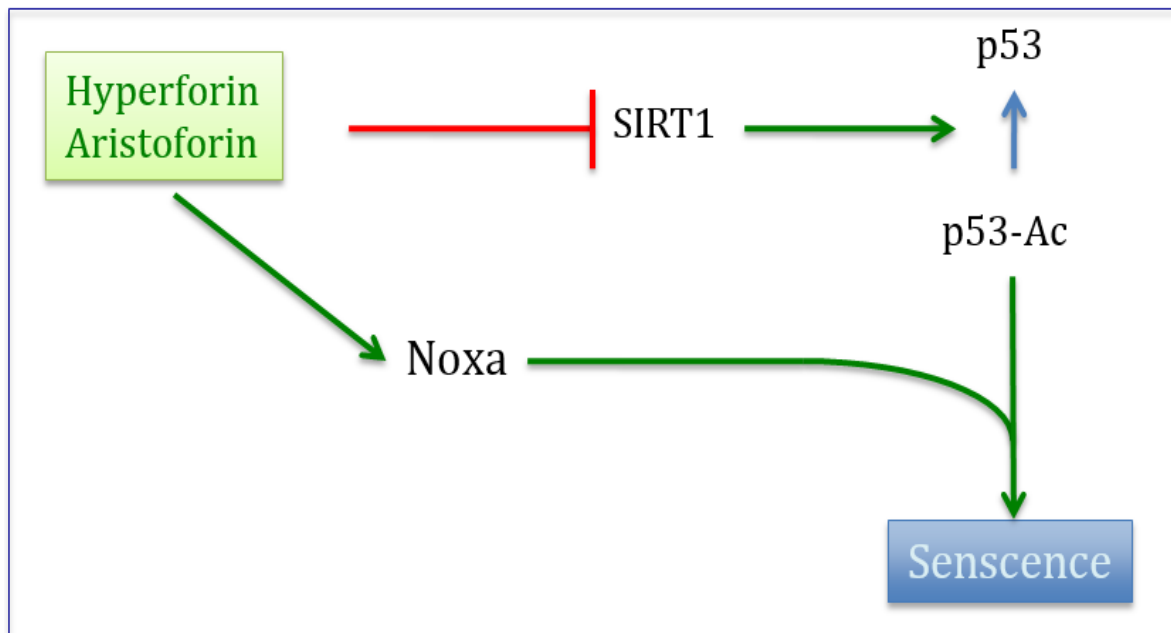


Figure 23 - Schematic representation of mechanisms through which hyperforin and aristoforin induce senescence

On one hand, hyperforin and aristoforin inhibit SIRT1, resulting in lower suppression of SIRT1-dependent deacetylation of p53. On the other hand, hyperforin and aristoforin induce Noxa expression, which also activates senescence, but only in the presence of p53.

5.2.1 Role of SIRT1

Several of my results indicate at least a partial role for hyperforin-induced suppression of SIRT1 in senescence induction. RSV stimulates SIRT1 activity (Howitz et al, 2003) and is able to rescue hyperforin- and aristoforin-induced senescence in both endothelial cells and some tumor cells (Figure 7, Figure 10). These data are consistent with the literature that shows decreased levels of SIRT1 are associated with growth arrest of tumors in vivo (Campisi, 2005) and increased senescence in endothelial progenitor cells (Potente et al, 2007).

In HUVECs and LECs my data show that RSV (10 μ M) reduces senescence induction in hyperforin, aristoforin and sirtinol-treated cells to baseline levels (Figure 12). This suggests that the main mechanism by which hyperforin induces senescence in these endothelial cells is dependent on SIRT1. In tumor cell lines with wild-type p53 such as HCT+/+ and MCF-7, hyperforin-induced senescence was also fully rescued by RSV. However, in cell lines with non-functional p53 (HCT-/-, PC3 and SW480),

hyperforin and aristoforin only marginally induced senescence. Furthermore, senescence induction was not reduced to baseline levels with RSV, in contrast to sirtinol-induced senescence in these cells (Figure 13). These results suggest that senescence induction via SIRT1 inhibition requires p53, and that a minority of senescence induction by hyperforin and aristoforin is p53- and SIRT1-independent.

Further evidence for SIRT1-independent hyperforin-induced senescence in p53 wildtype cells was obtained through SIRT1 knockdown. Although knockdown of SIRT1 sufficed to increase spontaneous senescence (Figure 15), hyperforin and aristoforin both further augmented senescence induction in SIRT1 knockdown cells. While it could be argued that knockdown of SIRT1 was incomplete, and thus that augmentation of senescence by hyperforin and aristoforin could be due to inhibition of the residual SIRT1 remaining after knockdown, note that the SIRT1 knockdown was highly efficient, and no SIRT1 protein could be detected by western blot (Figure 14). Thus I conclude that SIRT1 inhibition only partially accounts for hyperforin and aristoforin-induced senescence in both p53 wild-type and p53-deficient cells. Furthermore, in these experiments I observed that both hyperforin and aristoforin reduced the protein levels of SIRT1 relative to controls (Figure 15), suggesting that in addition to direct enzymatic inhibition of SIRT1 (Gey et al, 2007), hyperforin and aristoforin may also reduce SIRT1 activity at the expression level.

SIRT1 activity is increased in a variety of tumor types (Campisi, 2005) and plays an important role in DNA repair mechanisms (Oberdoerffer et al, 2008). Accordingly, SIRT1 has anti-senescence activities, which has been demonstrated in MCF-7 (breast cancer cells), H1299 (lung cancer cells), prostate cancer cells (Jung-Hynes, 2009) and HUVECs (Ota et al, 2007; Ota et al, 2008). During replicative or oncogene-induced senescence, inactivation of SIRT1 leads to increased levels of acetylated p53 (Pearson et al, 2000; Langley et al, 2002), the mechanism through which SIRT1 regulates senescence by p53 (Smith, 2002). Thus I predict that hyperforin and aristoforin treatment should lead to increased levels of acetylated p53 in those cells where hyperforin- and aristoforin-mediated inhibition of SIRT1 results in senescence.

5.2.2 Downstream targets: Noxa and p53

It has been reported that p53 promotes apoptosis by induction of BH3-only proteins such as Noxa and PUMA, for example as demonstrated in PUMA-null mice (Yu et al, 2003). In non-transformed cells, Noxa can mediate p53-dependent apoptosis, in a cell type-dependent manner (Quiney et al, 2006). On the other hand, Noxa induces cell cycle arrest at the G₀ phase of the cell cycle in chronic lymphatic leukemia (CLL) cells, resulting the resistance of these cells to apoptotic signals (Kolb et al, 2003). Hyperforin has been previously reported to induce Noxa expression in CLL cells (Zaher et al, 2009). Consistently, we also found that Noxa expression is induced by hyperforin in a dose-dependent manner in MCF-7 cells. The concentrations of hyperforin used were sufficient to induce senescence but not apoptosis. Importantly, knockdown of Noxa in these cells substantially attenuated hyperforin-induced senescence (Figure 18). These observations are novel in that while Noxa has previously been implicated in apoptosis induction, this is the first evidence that it also plays a role in senescence. Nevertheless, hyperforin and aristoforin did not significantly induce senescence in p53 deficient HCT cells, even though Noxa expression was induced in these cells (Figure 20). Thus p53 appears to be required for Noxa-induced senescence. Furthermore, Noxa expression is induced by hyperforin in the absence of p53 (Figure 20). These observations are also novel, as to date Noxa induction has been investigated in its context as a p53 response gene.

My results clearly show that p53 plays a central role in hyperforin and aristoforin-mediated senescence. In cells deficient in p53, hyperforin and aristoforin-induced senescence was substantially attenuated (Figure 10, Figure 20). Furthermore, Noxa-induced senescence was found to be dependent on p53 (Figure 20). The ability of RSV to suppress hyperforin-induced senescence was also dependent in part on the presence of p53 (Figure 13). Further work will be required to determine whether p53 levels remain unaffected by hyperforin, or whether hyperforin upregulates p53 or modifies its post-translational modification, for example through acetylation. These studies will cast further light on the role of p53 in hyperforin and aristoforin-induced senescence. Nevertheless it is clear from my studies that hyperforin and aristoforin can also induce senescence, albeit less effectively, in a p53-independent manner.

5.2.3 Perspectives

Future studies to further investigate hyperforin and aristoforin-induced senescence will be facilitated by the establishment of a method for quantifying senescent cells based in the use of MUG (Gary et al, 2005) that I show here is comparable with the traditional x-gal/FeCN assay (Dimri et al, 1995). The latter method is not sensitive enough to reveal the full range of SA- β -gal expression, and is very time consuming (Gugliotta et al, 1992; Kishigami et al, 2006). Thus the MUG method I describe here will have considerable advantages in terms of throughput, objectivity and accuracy. Nevertheless, the x-gal method has the advantage that the percentage of x-gal positive cells is quantified, whereas the MUG method only produces relative senescence values. However, if necessary this drawback could be overcome by producing a standard curve of MUG values plotted relative to x-gal values.

My results suggest that hyperforin clearly induces senescence through other targets in addition to SIRT1 and Noxa. In the context of p53-induced senescence, other downstream targets of p53 may be involved. For example p21 and PML, the p53 target genes, lead to oncogene-induced senescence (De Stanchina et al, 2004). Whether these p53 target genes contribute to senescence induction by hyperforin needs further investigation.

The data presented here add further support to the notion that hyperforin and its derivatives may have utility in the therapy of cancer by suppressing tumor growth. Nevertheless, the induction of senescence by these compounds that I demonstrate here suggests that caution may be needed when taking these substances to the clinic. In particular, the therapeutic induction of cellular senescence potentially has unwanted side effects. Firstly, the senescence-mediated decrease in the regenerative capacity of normal tissues results in aging (Campisi, 2005). Secondly, the induction of senescence can lead to the activation of the senescence-associated secretory phenotype (SASP), in which cytokines and other proinflammatory proteins become upregulated, and thereby disrupt normal tissue homeostasis and induce inflammation, which can act positively on tumor formation and promote degenerative or hyperproliferative changes in neighboring cells (Parrinello et al, 2005; Muller et al, 2009; Coppe et al, 2010). Thus while senescence-inducing compounds may on the one hand inhibit tumor growth by inducing senescence, on

the other hand they may promote tumor growth and progression if they induce an SASP. Future work will focus on whether hyperforin and its derivatives induce an SASP, and whether this limits the clinical application of these compounds.

6 REFERENCES

- Akiyama SK, Hasegawa E, Hasegawa T and Yamada KM** (1985). The interaction of fibronectin fragments with fibroblastic cells. J. Biol. Chem. 13256-13260.
- Alcorta DA, Y. Xiong, D. Phelps, G. Hannon, D. Beach, JC Barrett** (1996). Involvement of the cyclin-dependent kinase inhibitor p16 (INK4a) in replicative senescence of normal human fibroblasts. Proc. Natl Acad. Sci. USA. 13742-13747.
- Arfan M, Raziq N, Aljančić I, Milosavljević Sn** (2009). Secondary metabolites of *Hypericum monogynum* from Pakistan. Journal of the Serbian Chemical Society. 129–132.
- Alimonti A, Carrucedo A, Clohessy J, Trotma L, Nardella C, Egia A, Salmena L, Sampieri K, Pier PP** (2010). Subtle variations in Pten dose determine cancer susceptibility. Nature genetics. 454-458.
- Bakkenist CJ, Kastan MB** (2003). DNA damage activates ATM through intermolecular autophosphorylation and dimer dissociation. Nature. 499-506.
- Basu, T.N., D.H. Gutmann, J.A. Fletcher, T.W. Glover, F.S. Collins, and J. Downward** (1992). Aberrant regulation of ras proteins in malignant tumour cells from type 1 neurofibromatosis patients. Nature. 713–715.
- Beausejour, C, Krtolica A, Galimi F, Narita M, Lowe S, Yaswen Y, Campisi J** (2003). Reversal of human cellular senescence: roles of the p53 and p16 pathways. EMBO J. 4212–4222.
- Benhar M, Engelberg D and Levitzki A** (2002). ROS, stress-activated kinases and stress signaling in cancer. EMBO Reports. 420-425.
- Blagosklonny MV** (2008). Cell cycle arrest is not senescence. Cell Cycle. 94-101.
- Bodnar, A. G., Ouellette, M., Frolkis, M., Holt, S. E., Chiu, C. P., Morin, G. B., Harley, C. B., Shay, J. W., Lichtsteiner, S., and Wright, W. E** (1998). Extension of Life Span by Introduction of Telomerase into Normal Human Cells. Science. 349-352.
- Bond, J. A., F. S. Wyllie, and D. Wynford-Thomas** (1994). Escape from senescence in human diploid fibroblasts induced directly by mutant p53. Oncogene. 1885-1889.
- Bond, J.A., Haughton M., Blaydes J., Gire V., Wynford-Thomas D., Wyllie F.** (1996). Evidence that transcriptional activation by p53 plays a direct role in the induction of cellular senescence. Oncogene. 2097–2104.
- Bordone L, Motta MC, Picard F, Robinson A, Jhala US, Apfeld J, McDonagh T, Lemieux M, McBurney M, Szilvasi A, Easlon EJ, Lin SJ, Guarente L** (2006). Sirt1

Regulates Insulin Secretion by Repressing UCP2 in Pancreatic β Cells. PLOS biology. 31.

Bunz F., Hwang P.M., Torrance C., Waldman T., Zhang Y., Dillehay L., Williams J., Lengauer C., Kinzler K.W. and Vogelstein B. (1999). Disruption of p53 in human cancer cells alters the responses to therapeutic agents. JCI. 263-269.

Caldecott KW (2008). Single-strand break repair and genetic disease. Nature Reviews Genetics. 619-631.

Campisi, J. (2001). Cellular senescence as a tumor-suppressor mechanism. Trend cell Bio. 27-31.

Campisi, J. (2005). Suppressing cancer: the importance of being senescent. Science. 886–887.

Campisi J, FA di Fagagna (2007). Cellular senescence: when bad things happen to good cells. Nature Reviews Molecular Cell Biology. 729-740.

Campisi J., Dimri, G.P. & Hara (1996). Control of replicative senescence. In Handbook of the Biology of Aging. Wiley-Liss, New York. 348-373.

Canman, CE, Wolff, AC, Chen, CY, Fornace, AJ & Kastan, MB (1994.) The p53-dependent G1 cell cycle checkpoint pathway and ataxia-telangiectasia. Cancer Res. 5054–5058.

Carmeliet P and Jain RK (2000). Angiogenesis in cancer and other diseases. Nature. 249-257.

Carnes BA, Olshansky SJ (1994). Evolutionary perspective on human senescence. Population and Development Review. 57-80.

Casley-Smith, J.R., Reade P.C. (1961). The Properties of Endothelium. Brit.J.exp.Path. 473-480.

Chen Q., Fischer, A., Reagan, J. D., Yan, L. J. & Ames, B.N. (1995). Damage and senescence of human diploid fibroblast cells. Proc. Natl. Acad. Sci. USA. 4337–4341.

Chen, Z., Trotman, L.C., Shaffer, D., Lin, H.K., Dotan, Z.A., Niki, M., Koutcher, J.A., Scher, H.I., Ludwig, T., Gerald, W., et al. (2005). Crucial role of p53-dependent cellular senescence in suppression of Pten-deficient tumorigenesis. Nature. 725-730.

Cho, KA, Ryu SJ, Oh YS, Park JH, Lee JW, Kim HP, Kim KT, Jang IS, Park SC (2004). Morphological Adjustment of Senescent Cells by Modulating Caveolin-1 Status. Journal of Biological. 42270-42278.

Chu F., Chou PM, Zheng X, Mirkin BL, Rebbaa A (2005). Control of multidrug resistance gene *mdr1* and cancer resistance to chemotherapy by the longevity gene *sirt1*. Cancer Res. 10183-7.

Costanzi C and Pehrson JR (1998). Histone macroH2A1 is concentrated in the inactive X chromosome of female mammals. Nature. 599–601.

Courtois-Cox,S, GentherWilliams SM, Reczek EE, JohnsonBW, McGillicuddy LT, Johannessen CM(2006). A negative feedback signaling network underlies oncogene-induced senescence. Cancer cell. 459–472.

Dagert, M. & Ehrlich, S. D. (1979). Prolonged incubation in calcium chloride improves the competence of *Escherichia colicells*. Gene. 23-28.

Delia D, Aiello A, Formelli F, Fontanella E. Costa A, Miyashita T, Reed JC, Pierott MA (1995). Regulation of apoptosis induced by the retinoid N-(4-hydroxyphenyl) retinamide and effect of deregulated bcl-2. Blood. 359-367.

Dexter, DL, Barbosa, JA &Calabresi(1979). N, N-Dimethylformamide induced alteration of cell culture characteristics and loss of tumorigenicity in cultures of human colon carcinoma cells. Cancer Res.1020-1025.

Gary RK, Kindell SM (2005). Quantitative assay of senescence-associated beta-galactosidase activity in mammalian cell extracts. Anal Biochem. 329–334.

Gey C., Kyrylenko, S., Hennig, L., Nguyen, L.-Hoa D., Büttner, A., Pham, Hung D. and Giannis, A. (2007). Phloroglucinolderivate Guttiferon G, Aristoforin und Hyperforin: Inhibitoren der menschlichen Sirtuine SIRT1 und SIRT2. Angewandte Chemie. 5311–5314.

Giaccia AJ, and KastanMB (1998). The complexity of p53 modulation: emerging patterns from divergent signals. Genes & Dev.2973– 2983.

Goyette MC, Cho K, Fasching CL, Levy DB, Kinzler KW, Paraskeva C, Vogelstein B, Stanbridge EJ (1992). Progression of colorectal cancer is associated with multiple tumor suppressor gene defects but inhibition of tumorigenicity is accomplished by correction of any single defect via chromosome transfer. Molecular and cellular biology. 1387-1395.

Grozinger CM, Chao ED, Blackwell HE, Moazed D, Schreiber SL(2001). Identification of a class of small molecule inhibitors of the sirtuin family of NAD-dependent deacetylases by phenotypic screening. J. Biol. Chem. 38837–38843.

Gugliotta P., Pacchioni D., Bussolati G. (1992). Staining reaction for beta-galactosidase in immunocytochemistry and in situ hybridization. Eur. J. Histochem. 143-148.

Hara E, Smith R, Parry D, Tahara H, Stone S, Peters G (1996). Regulation of p16/CDKN2 expression and its implications for cell immortalization and senescence. Mol. Cell. Biol. 859-867.

Harley CB (1991). Telomere loss: mitotic clock or genetic time bomb? Mutation Research/DNAging. 271–282.

Hay, R.J and Strehler, B.L (1967). The limited growth span of cells strains isolated from the chicken embryo. Exp. Gerontol. 123-135.

Hayflick L (1965). The limited in vitro lifetime of human diploid strains. Exp Cell Res. 614-635.

Hayflick L and Moorhead PS (1961). The serial cultivation of human diploid cell strains. Exp. Cell Research. 585-621.

Herbig, U., Jobling, W. A., Chen, B. P., Chen, D. J., and Sedivy, J. M. (2004). Telomere shortening triggers senescence of human cells through a pathway involving ATM, p53 and p21, but not p16INK4. Molecular Cell. 501-513.

Hoeijmakers JHJ (2009). DNA Damage, Aging, and Cancer. New England Journal of Medicine. 1475-1485.

Hölzl J (1993). Inhaltsstoffe und Wirkmechanismen des Johanniskrautes. Phytoter. 255-264.

Howitz, K .T., Bitterman, K.J., Cohen, H.Y., Lamming, D.W., Lavu, S., Wood, J.G., Zipkin, R.E., Chung, P., Kisielewski, A., Zhang, L.L., et al. (2003). Small molecule activators of sirtuins extend *Saccharomyces cerevisiae* lifespan. Nature. 191–196.

Huffman DM, Grizzle WE, Bamman MM (2007). SIRT1 is significantly elevated in mouse and human prostate cancer. Cancer Res. 6612-8.

Iyer, VN& Szybalski, W. (1964). Mitomycins and porfiromycin: chemical mechanism of activation and cross-linking of DNA. Sceince. 55-58.

Jaff EA, NACHMAN RL, BECKER CG, MINICK CR (1973). Culture of human endothelial cells derived from umbilical veins. Identification by morphologic and immunologic criteria. J Clin Invest. 2745-2756.

Jiricny J (2006). The multifaceted mismatch-repair system. Nature Reviews Molecular Cell Biology. 335-346.

Kauffmann-Zeh, A., Rodriguez-Viciana, P., Ulrich, E., Gilbert, C., Cof- fer, P., Downward, J., and Evan, G. (1997). Suppresion of c-Myc-induced apoptosis by ras signalling through PI(3)K and PKB. Nature. 544-548.

Keller JN, Dimayuga E, Chen Q, Thorpe J, Gee J, Ding Q. (2004). Autophagy, proteasomes, lipofuscin, and oxidative stress in the aging brain. ScienceDirect. S. 2376–2391.

Kemp, C., Donehower, LA, Bradley, A. & Balmain, A. (1993). Reduction of p53 gene does not increase initiation or promotion but enhances malignant progression of chemically induced skin tumors. Cell. 813–822.

Kishigami S., Komatsu Y., Takeda H., Nomura-Kitabayashi A., Yamauchi Y., Abe K., Yamamura K., Mishina Y. (2006). Optimized beta-galactosidase staining method for simultaneous detection of endogenous gene expression in early mouse embryos. Genesis. 57-65.

Kiyono T, Foster SA, Koop JI, McDougall DA, KlingelhutzAJ (1998). Both Rb/p16INK4a inactivation and telomerase activity are required to immortalize human epithelial cells. Nature. 84-88.

Korotchkina LG, Leontieva OV, Bukreeva EI, et al. (2010). The choice between p53-induced senescence and quiescence is determined in part by the mTOR pathway. Aging. 344–352.

Kracikova M, Akiri G, George A, Sachidanandam R and Aaronson SA (2013). A threshold mechanism mediates p53 cell fate decision between growth arrest and apoptosis, Cell Death & Differentiation. 576-588.

Laemmli, U.K. (1970). Cleavage of structural proteins during the assembly of the head of bacteriophage T47. Nature London. 680-685.

Land H., Parada, LF & Weinberg, RA (1983). Tumorigenic conversion of primary embryo fibroblasts requires at least two cooperating oncogenes. Nature. 596–602.

Lee, YJ, CS. Kim and D.K. Oh (2004). Lactulose production by β -galactosidase in permeabilized cells of *Kluyveromyces fragilis*. Applied Microbiol. Biotechnol. 787-793.

Lima L., and Macieira-Coelho A. (1972). Parameters of aging in chicken embryo fibroblasts cultivated. Exp. Cell Res. 279-284.

Lin, AW, Barradas M, Stone JC, van Aelst L, Serrano M & Lowe SW (1998). Premature senescence involving p53 and p16 is activated in response to constitutive MEK/MAPK mitogenic signaling. Genes & Development. 3008-3019.

Lindahl T (2000). Suppression of spontaneous mutagenesis in human cells by DNA base excision–repair. Mutation Research/Reviews in Mutation Research. 129–135.

Liu G, Yuan X, Zeng Z, Tunici P, Ng H, Abdulkadir IR, Lu L, Irvin D, Black KL, Yu JS (2006). Analysis of gene expression and chemoresistance of CD133+ cancer stem cells in glioblastoma. Mol Cancer. 67.

Mallette FA, Gaumont-Leclerc MF, Ferbeyre G. (2007). The DNA damage signaling pathway is a critical mediator of oncogene-induced senescence. Gene & Dev. 43-48.

Martelli AM, Nyakern M, Tabellini G, Bortul R, Tazzari PL, et al. (2006). Phosphoinositide 3-kinase/Akt signaling pathway and its therapeutic implications for human acute myeloid leukemia. Leukemia. 911-928.

Matsumura, T., Zerrudo, Z., & Hayflick, L. (1979). Senescent human diploid cells in culture: survival, DNA synthesis and morphology. Journal of Gerontology. 328-334.

Medcalf AS, Klein-Szanto AJ, Cristofalo VJ (1996). Expression of p21 is not required for senescence of human fibroblasts. Cancer Res. 4582-4585.

Medina MA, Martínez-Poveda B, Amores-Sánchez MI, Quesada AR (2006). Hyperforin: More than an antidepressant bioactive compound? Life sciences. 105–111.

Merhi F, Tang R, Piedfer M, Mathieu J, Bombarda I, et al. (2011). Hyperforin Inhibits Akt1 Kinase Activity and Promotes Caspase-Mediated Apoptosis Involving Bad and Noxa Activation in Human Myeloid Tumor Cells. PLOS one. 25963.

MoldovanGL, D'Andrea AD (2009). How the Fanconi Anemia pathway guards the genome. Annual review of genetics. 223-249.

Muller M (2009). Cellular senescence: Molecular mechanism, in vivo considerations. Antioxidants and redox signaling. 59-98.

Nagafuchi A and Takeichi M (1989). Transmembrane control of cadherin mediated cell adhesion: a 94 kDa protein functionally associated with a specific region of the cytoplasmic domain of E-cadherin. Cell Regul. 37-44.

Narita M (2007). Cellular senescence and chromatin organisation. Nature. 686–691.

Narita, M, Núñez S, Heard E, Narita M, Lin AW, Hearn SA, Spector DL, Hannon GJ, Lowe SW. (2003). Rb-mediated heterochromatin formation and silencing of E2F target genes during cellular senescence. Cell. 703–716

Nicke, J.B., Khanna, S.J., Warne, P.H., Cowling, V., Cook, S.J., Peters, G., Delpuech, O., Schulze, A., Berns, K., Mullenders, J., Beijersbergen, R.L., Bernards, R., Ganesan, T.S., Downward, J. and Hancock, D.C. (2005). Involvement of MINK, a Ste20 Family Kinase, in Ras Oncogene-Induced Growth Arrest in Human Ovarian Surface Epithelial Cells. Molecular Cell. 673–685.

Noonan DM, Sogno I, Albin A (2011). 16 plants and plant-driven products as cancer chemopreventive agent. Springer: New York. 57–75.

Oberdoerffer P, Michan S, McVay M, Mostoslavsky R, Vann J, Park SK, Hartlerode A, Stegmuller J, Hafner A, Loerch P, Wright SM, Mills KD, Bonni A, Yankner BA, Scully R, Prolla TA, Alt FW, Sinclair DA (2008). SIRT1 redistribution on chromatin promotes genomic stability but alters gene expression during aging. Cell. 907–918.

Olovnikov, Ivan A.; Kravchenko, Julia E.; Chumakov, Peter M(2009). Homeostatic functions of the p53 tumor suppressor: Regulation of energy metabolism and antioxidant defense. ScienceDirect. 32–41.

O'Shea C, Crompton T, Rosewell IR, Hayday AC, and Owen MJ (1996). Raf regulates positive selection. Eur. J. Immunol. 2350-2355.

Ota H, Akishita M, Eto M, Iijima K, Kaneki M, Ouchi Y. (2007). Sirt1 modulates premature senescence-like phenotype in human endothelial cells. J. Mol. Cell Cardiol. 571-579.

Palmero, C.Pantoja, M. Serrano (1998). P19ARF links the tumour suppressor p53 to Ras. Nature. 125–126.

Parrinello S, Samper E, Krtolica A, Goldstein J, Melov S, Campisi (2003). Oxygen sensitivity severely limits the replicative lifespan of murine fibroblasts. Nat Cell Bio. 741–747.

Parrinello S, Coppe JP, Krtolica A and Campisi J (2005). Stromal-epithelial interactions in aging and cancer: senescent fibroblasts alter epithelial cell differentiation. Journal of cell. 485-496.

Poele te RH, Okorokov AL, Jardine L, Cummings J and Joel SP.(2002). DNA damage is able to induce senescence in tumor cells in vitro. Cancer Research. 1916-1930.

Potente , M., Ghaeni, L., Baldessari, D., Mostoslavsky, R., Rossig, L., Dequiedt, F., Haendeler, J., Mione, M., Dejana, E., Alt, F.W., et al. 2007). SIRT1 controls endothelial angiogenic functions during vascular growth. Genes Dev. 2644–2658.

Prowse K.R., and Greider, C.W. (1995). Developmental and tissue-specific regulation of mouse telomerase and telomere length. PNAS. 4818–4822.

Qian Y and Chen X(2013). Senescence regulation by the p53 protein family. Cell senescence. 37-61.

Quiney C, Billard C, Faussat AM, Salanoubat C, Ensaf A, Nait-Si Y et al. (2006). Pro-apoptotic properties of hyperforin in leukemic cells from patients with B-cell chronic lymphocytic leukemia. Leukemia . 491–497.

Robles, S. J., and Adami, G.R. (1998). Agents that cause DNA double strand breaks lead to p16INK4a enrichment and the premature senescence of normal fibroblasts. Oncogene. 1113–1123.

Rothley M, Schmid A, Thiele W, Schacht V, Plaumann D, Gartner M, Yektaoglu A, Bruyère F, Noël A, Giannis A, Sleeman JP. (2009).Hyperforin and aristoforin inhibit lymphatic endothelial cell proliferation in vitro and suppress tumor-induced lymphangiogenesis in vivo. Journal of Cancer. 34–42.

Samorajski T. and J. MF. Ordy and P. Rady- Reimer.(1968). Lipofuscin Pigment Accumulation in the Nervous System of Aging Mice. Anat. Rec. 555-574.

Sasaki, T., Maier, B., Bartke, A. and Scrable, H.(2006). Progressive loss of SIRT1 with cell cycle withdrawal. Aging Cell. 413–422.

Schempp CM, Kirkin V, Simon-Haarhaus B, Kersten A, Kiss J, Termeer CC et al. (2002). Inhibition of tumour cell growth by hyperforin, a novel anticancer drug from St. John's wort that acts by induction of apoptosis. Oncogene. 1242–1250.

Schempp CM, Pelz K, Wittmer A, Schopf E, Simon (1999). Antibacterial activity of hyperforin from St John's wort, against multiresistant Staphylococcus aureus and gram-positive bacteria. Lancet. 2129.

Schempp CM, Winghofer B, Lüdtke R, Haarhaus BS, Schöpf E, Simon JC (2000). Topical application of St John's wort (*Hypericum perforatum* L.) and of its metabolite hyperforin inhibits the allostimulatory capacity of epidermal cells. British Journal of dermatology. 979–984.

Serrano M, Lin AW, McCurrach ME, Beach D, Lowe SW (1997). Oncogenic ras Provokes Premature cell senescence associated with accumulation of p53 and p16INK4a. Cell. 593–602.

Shay JW & Roninson IB (2004). Hallmarks of senescence in carcinogenesis and cancer therapy. Oncogene. 2929-33.

Shay WE & Wright JW (2005). Senescence and immortalization: role of telomeres and telomerase. Carcinogenesis. 867-874.

Sherr, C.J. and DePinho, R.A. (2000). Cellular senescence: Mitotic clock or culture shock? Cell. 407–410.

Sherwood SW, Rush D, Ellsworth JL, Schimke (1988). Defining cellular senescence in IMR-90 cells: a flow cytometric analysis. Proc Natl Acad Sci U S A. 9086-90.

Smith S (2002). Human Sir2 and the ‘silencing’ of p53 activity. ScienceDirect. 404–406.

Tissenbaum HA &Guarente, L. (2001). Increased dosage of a sir-2 gene extends lifespan in *Caenorhabditis elegans*. Nature. 227-230.

Vigneron A, Vousden KH (2010). P53, ROS and senescence in the control of aging. Aging (Albany NY). 471–474.

Vogel G., Thorin-Trescases N., Farhat N., et al. (2007) Cellular senescence in endothelial cells from atherosclerotic patients is accelerated by oxidative stress associated with cardiovascular risk factors. Mech Ageing Dev. 662-671.

Wood J.G., Rogina, B., Lavu, S., Howitz, K., Helfand, S.L., Tatar, M., and Sinclair, D (2004). Sirtuin activators mimic caloric restriction and delay ageing in metazoans. Nature. 686-689.

Xu Y, Li N, Xiang R, Sun P (2014). Emerging roles of the p38 MAPK and PI3/AKT/mTOR pathways in oncogene-induced senescence. Trend Biochem Sci. 268-276.

Yi J, Luo J (2010). SIRT1 and p53, effect on cancer, senescence and beyond. ScienceDirect. 1684–1689.

Young, AR, Narita M, Ferreira M, Kirschner K, Sadaie M.(2009). Autophagy mediates the mitotic senescence transition. Genes & Development. 798-803.

Yu, J., wang, Z., K.W., Vogelstein, B., and Zhang, L. (2003). PUMA mediates the apoptotic response to p53 in colorectal cancer cells. Proc. Natl. Acad. Sci. USA. 1931-1936.

Zaher M, Akrouf I, Mirshahi M, Kolb JP, Billard (2009). Noxa upregulation is associated with apoptosis of chronic lymphocytic leukemia cells induced by hyperforin but not flavopiridol. Leukemia. 594–596.

Zanke B .W., Boudreau, K., Rubie, E., Winnett, E., Tibbles, L.A., Zon, L., Kyriakis, J., Liu, F.F., and Woodgett, J.R. (1996).The stress-activated protein kinase pathway mediates cell death following injury induced by cis-platinum, UV irradiation or heat .ScienceDirect. 606-613.

Zhang, R., M. V. Poustovoitov, X. Ye, H. A. Santos, W. Chen, S. M. Daganzo, J. P. Erzberger, I. G. Serebriiskii, A. A. Canutescu, R. L. Dunbrack, J. R. Pehrson,

J. M. Berger, P. D. Kaufman, and P. D. Adams. (2005). Formation of MacroH2A-containing Senescence-Associated Heterochromatin Foci and Senescence Driven by ASF1a and HIRA. Developmental cell. 19–30.

Zhao S, Konopleva M, Cabreira-Hansen M, Xie Z, Hu W, et al. (2004). Inhibition of phosphatidylinositol 3-kinase dephosphorylates BAD and promotes apoptosis in myeloid leukemias. Leukemia. 267-275.

Zhu J., Woods, D., McMahon, M. & Bishop, JM (1998). Senescence of human fibroblasts induced by oncogenic Raf. Genes Dev. 2997–3007.

7 ACKNOWLEDGEMENT

First of all, I thank my supervisor, professor Sleeman, who helped me patiently to complete my thesis and was always there to answer my questions. Thank you very much for all the things you taught me.

I also thank the second supervisor, professor Foulkes, whose great ideas helped this thesis.

I thank my dear colleague, Dr. Susanne Hausselt, who dedicated a lot of time to complete this thesis and his presence was very effective to me.

I thank all my colleagues at Labor for the lovely environment they have created, especially Anke, Gitta, Anne, Vanessa, Annette, Sonja, Justyna and Luca who made good and memorable hours for the group.

I thank my dear friends Ludmila, Andrey and Amanda for finding the literature.

I thank my dear parents who made this path possible, and supported me. I love them.

But it was one who helped me all the way to the end, tried hard and I could rely on. I cannot find proper words to thank him. I can only say: "I love you, my dear husband, Arash. Without your help I couldn't be where I am now. Thank you for being there."

Halfway, a little man joined me and his little fantastic world calmed me down. "I love you, my beloved Paya. You were the God's gift to us."